CHALMERS

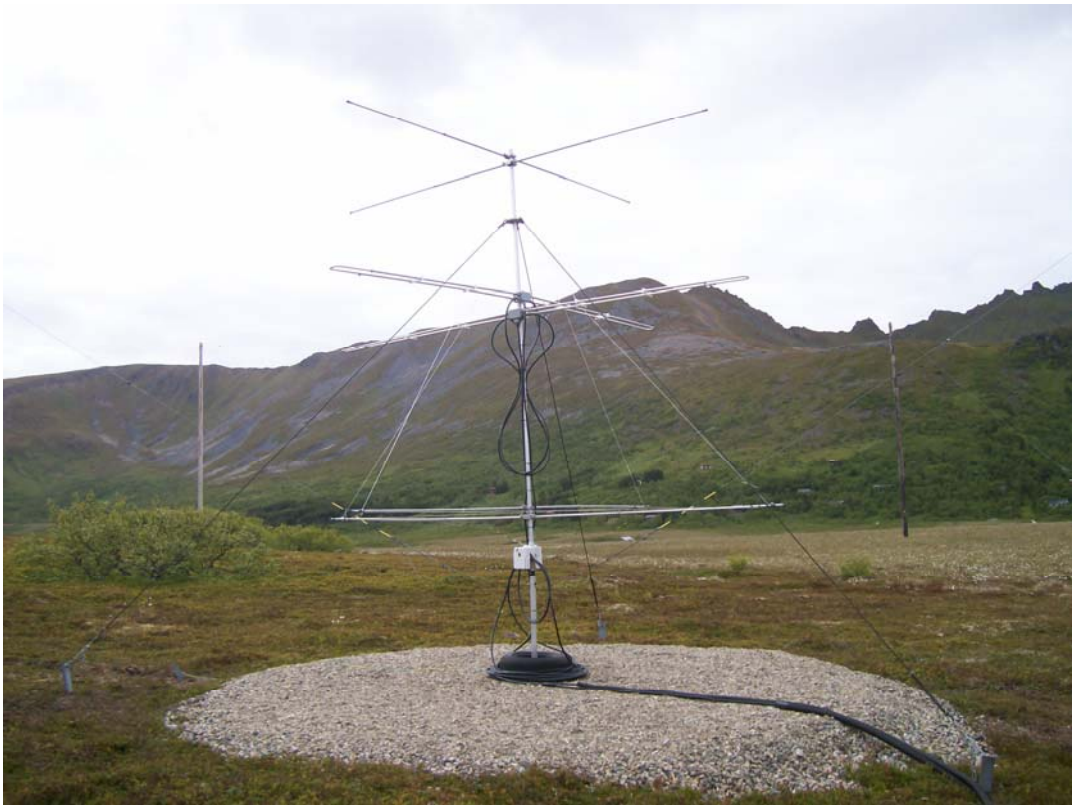

Experimental study of the influences of background atmospheric electron density on radar backscatter from meteor trails

Master of Science Thesis

DING TAO

Department of Radio and Space Science

CHALMERS UNIVERSITY OF TECHNOLOGY

Gothenburg, Sweden 2010

Experimental study of the influences of background atmospheric electron density on radar backscatter from meteor trails

DING TAO

Department of Radar Soundings and Sounding Rockets
Leibniz Institute of Atmospheric Physics (IAP)
Kühlungsborn, Germany

Department of Radio and Space Science
CHALMERS UNIVERSITY OF TECHNOLOGY
Gothenburg, Sweden 2010

Experimental study of the influences of background atmospheric electron density on radar backscatter from meteor trails

DING TAO

Supervisor:
Dr. Werner Singer
Leibniz Institute of Atmospheric Physics (IAP)
Kühlungsborn 18225
Germany

Examiner:
Dr. Leif Eriksson
Department of Radio and Space Science
Chalmers University of Technology
SE-412 96 Gothenburg
Sweden
Telephone + 46 (0)31-772 1000

Cover:
A photograph shows the transmitting antenna of the SKiYMET radars.
Credit: Ding Tao, Andenes, Norway, June 21, 2009.

Gothenburg, Sweden 2010

“夏四月辛卯夜，恒星不见，夜中星陨如雨。”

——《左传》，公元前 687 年

Acknowledgements.

This thesis was performed at the Leibniz Institute for Atmospheric Physics (IAP), Kühlungsborn, Germany. I would like to deeply thank my supervisor Dr. Werner Singer, for his invaluable help and guidance. And I am truly indebted to my colleagues at IAP, especially Prof. Markus Rapp, Dr. Norbert Engler, Manja Placke and Qiang Li for their support in all aspects. The help from my examiner Dr. Leif Eriksson and all people at Department of Radio and Space Science, Chalmers University of Technology are also appreciated very much. Lastly I am sincerely grateful to Xiaojin Qiu, my family and friends.

Ding Tao

Gothenburg, April 2010

Experimental study of the influences of background atmospheric electron density on radar backscatter from meteor trails

DING TAO

Department of Radio and Space Science

Chalmers University of Technology

Abstract

Meteoroids entering the atmosphere burn up due to friction and form ionized meteor trails at altitudes between 70 km and 120 km approximately. The ionized trails can be detected by radar. Radar measurements have allowed determination of characteristics of both the meteor trails and the atmosphere around the trails. The measured meteor trail decay time is related with the ionized trail's expansion and the diffusion effects in the atmosphere, which could be used to estimate the neutral gas temperature of the atmosphere at the altitudes of the meteor layer.

This thesis examines one possible influence on meteor decay times, the background atmospheric electron density variations. At the main meteor layer (about 50 to 95 km above Earth's surface), the ionosphere electron density varies between daytime and nighttime. The meteor decay time dependency on solar zenith angle, time of year and altitude were studied to understand the relation between meteor decay time behaviour and background atmospheric electron density variations. The meteor data came from meteor radar observations at the frequencies 32.55 MHz and 53.5 MHz, at mid-latitude 54°N (Juliusruh, Germany) and polar latitude 69°N (Andenes, Norway), during the year 2008. The influence of meteor decay time variation on the atmosphere temperature estimations is also discussed.

Keywords: Meteor, Meteor radar, Ambipolar diffusion, Decay time, Electron density, Atmospheric temperature

Contents

1 Introduction

At every moment, many meteoroids enter the Earth's atmosphere and burn up at altitudes from approximately 120 km down to 70 km. Then the meteor trails form and expand quickly, which can be detected by radars. The meteor decay times from radar observations represent the character of the trails expansion. The meteor studies show strong connection between meteor trails and the atmosphere around the trails, which provide a better understanding of the Earth's atmosphere, e.g. temperature, pressure, wind velocity, etc.

There are two kinds of meteor trails, underdense and overdense, defined by their electron line densities. Currently, the ambipolar diffusion is assumed to be the most significant mechanism for the underdense meteor trails expansion at Mesosphere and Lower Thermosphere (MLT). Model research deduces that there are two possible influences on the meteor trails expansion: the neutral or positively charged background dust and the background atmospheric electron density variation.

Havnes and Sigernes (2005) analyzed the decay time of underdense trails, which can be affected by a part of the trail electrons being absorbed by dust as the trail expands. Later, Singer et al. (2008) tested this background dust influence for the radar backscatter from underdense meteors by comparing the weak meteor echoes with strong meteor echoes. And there were more studies about this topic, which show approximately the same results, more background dust (neutral or positively charged) will absorb the meteor trail electrons, and then decrease the meteor decay times.

This thesis is the continued study of the possible influences on the meteor trails expansion, focusing on the effect of background atmospheric electron density variation.

Continuous all-sky radar observations of meteors during the year 2008, in mid-latitudes at Juliusruh, Germany (54°N) and in polar latitudes at Andenes, Norway (69°N) provide a substantial data set for efficient investigations of meteor decay times at different altitudes, time of day and month of year. The meteor data have been processed by Ding Tao at Leibniz Institute of Atmospheric Physics, to look for differences in decay times with the background ionization effects and its relevance for the temperature estimation from meteor trail decay times. The work for this thesis includes the basic overall meteor study (meteor flux, meteor rates, meteor height distributions, etc.), the meteor decay time study, the D-region ionosphere electron density variation comparison, the atmospheric temperature estimation.

Outline of the thesis

This thesis attempts to give an overall impression of the meteor phenomenon in Earth's atmosphere, investigate the radar backscatter from meteor trails, and quest the possible influences due to the background atmospheric electron density variation. In Sect. 2, the basic theory of meteors, Earth's atmosphere and the relationship between them are summarized. Sect. 3 is mainly about the radar observations of meteors, covering the experimental study details. Sect. 4 proceeds with the data analysis and results, including basic meteor data analysis, background atmospheric electron density study,

daytime/nighttime meteor decay time variation study, and atmospheric temperature estimations from meteor observations. Discussion, conclusions and some open issues for future research are presented at the end of the thesis.

2 Meteors and the Earth's atmosphere

2.1 Meteors

From ancient to modern time, meteors ("shooting stars") are one of the most mysterious miracles in the sky and many records can be found in the history, amateur and scientific. The space between the planets is filled with thousands of particles traveling at high speed relative to the Earth, called meteoroids. Meteoroids impinge the Earth's atmosphere with a typical speed between 11 and 72 km/s. Despite its size is usually small, it carries a notably large kinetic energy. This energy and its substance are dissipated in a brief blaze by collisions with the atoms and molecules in the atmosphere. The collisional process is normally just a few tenths of a second. This is known as a meteor phenomenon. Fast meteors with entry velocities higher than about 35 km/s burn up above 90 km and others with lower velocities burn up below 90 km. Meteor trails are the radiation emitted behind the meteor body ("meteor head") for seconds or more.

In more details, the process of meteoroids interaction with the atmosphere can be distinguished in the following 5 stages, orbital motion (meteoroid motion), preheating, ablation, dark-flight and impact. Note that ionization is a very important phenomenon, during the preheating and the ablation part of the trajectory.

Preheating is caused by the impacting molecules of the gas in the atmosphere, when the meteor body impinges the Earth atmosphere at heights of 300 to 100 km. This phenomenon lasts only seconds or tens of seconds. The surface temperature of the meteoroid rises rapidly. The next stage of atmospheric penetration of the meteoroid is ablation, which starts as destruction at the lower temperatures. After that, the final process of ablation is the evaporation from the body and its fragments with temperatures close to 2500 K. Then most of the kinetic energy is spent in the ablation process, so the temperatures will not further increase. In the end, there are not enough hot gases round the body to emit visible light, called dark-flight. (Ceplecha, Borovicka, Elford, Revelle, Hawkes, Porubcan, and Simek 1998) Very rarely, the residual debris of a large meteoroid may survive the fiery plunge and fall down to the ground as a *meteorite*, commonly breaking up into many small pieces. (McKinley 1961)

2.2 Meteor trails

Every meteor creates a train of excited and ionized atoms, called meteor trails. These atoms are slowed down to ordinary thermal velocities and expand behind the meteor head. The intensity of the meteor trail luminosity is much less than of the head and its decay is determined mainly by diffusion, recombination, and attachment. The initial trail width (the apparent width of the luminosity at the meteor head) is difficult to measure, and estimates vary widely from several tens of meters down to a few centimeters. Long-duration trails, lasting from a few seconds to many minutes, are usually linked to the brighter meteors and fireballs.

The kinetic energy of the meteoroid is converted to heat, light, and ionization by the collisions with air particles in the atmosphere. Atoms of the meteoroid are vaporized from the surface of the meteoroid body and the kinetic energy is more than adequate to excite and also to ionize the atoms of the meteor.

Light bursts are often observed, and occasionally the trail will appear to split into two or more slightly diverging trails as the meteoroid breaks into fragments. Below about 50 km sounds may be heard, first the sharp crack of the shock wave created by the supersonic motion and then a rumbling sound similar to thunder goes through the atmosphere. These sounds travel at a speed near 330 m/s, so several minutes may elapse between the passage of the meteor and the arrival of the sound. (McKinley 1961)

2.3 Meteor characteristics

Most meteors do not belong to any recognized meteor showers, named sporadic meteors. A meteor shower is mainly observed when the Earth passes through a meteoroid stream. The meteoroid streams are formed when the meteoroids are separated from the surface of a parent body. According to modern research, comets are believed to be the majority of parent bodies, though a few meteoroid streams are linked to asteroids. Most commonly, meteoroid streams are formed when dust is lifted from the surface of a comet by sublimating ice gas pressure as the comet passes close to the sun. Also, they may be formed from asteroids by such processes as collisions, rotational bursting, or tidal disruption. Many systematic studies about the meteor shower and sporadic meteors have been done by J. Jones and P. Brown (1993) and M. Campbell-Brown (2007).

Normally, during the year, the meteor count rates can vary between 100 and 500 meteors per hour approximately. In everyday measurements (24 hours), a maximum meteor number appears around dawn, and after dusk the meteor rate is the lowest. The main reason for this phenomenon is because of the Earth’s rotation. Very briefly, everyday before dawn, the Earth’s atmosphere can catch up more meteoroids. And after dusk, only a few faster meteors can impinge into the Earth’s atmosphere. The phenomenon is shown in Figure 2.1. (Singer, Bremer, Weiß, Hocking, Hoffner, Donner, and Espy 2004a; Singer, Zahn, and Weiß 2004b)

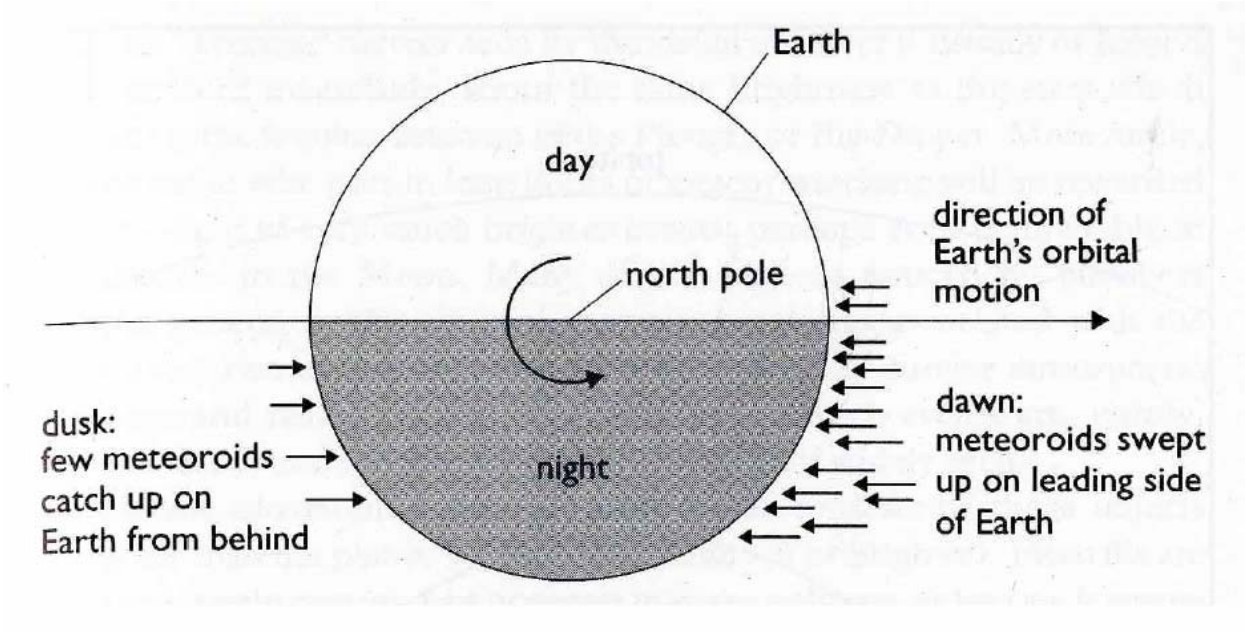

Figure 2.1 Hourly meteor rates variation principle

The following 3D plot (Figure 2.2) shows the meteor rates obtained with meteor radar on 32.55 MHz at mid-latitude 54°N (Juliusruh) 2008. From this figure, a clear (blue) valley is found, which shows the lowest meteor rates per day. This result matches the hourly meteor rates variation principle mentioned before. Note that the meteor data used here were selected by some criteria. The total meteor rates (without data selections) could be at least 50% higher than the data shown in the figure. The details of the meteor data selections will be discussed in Sec. 4.1.

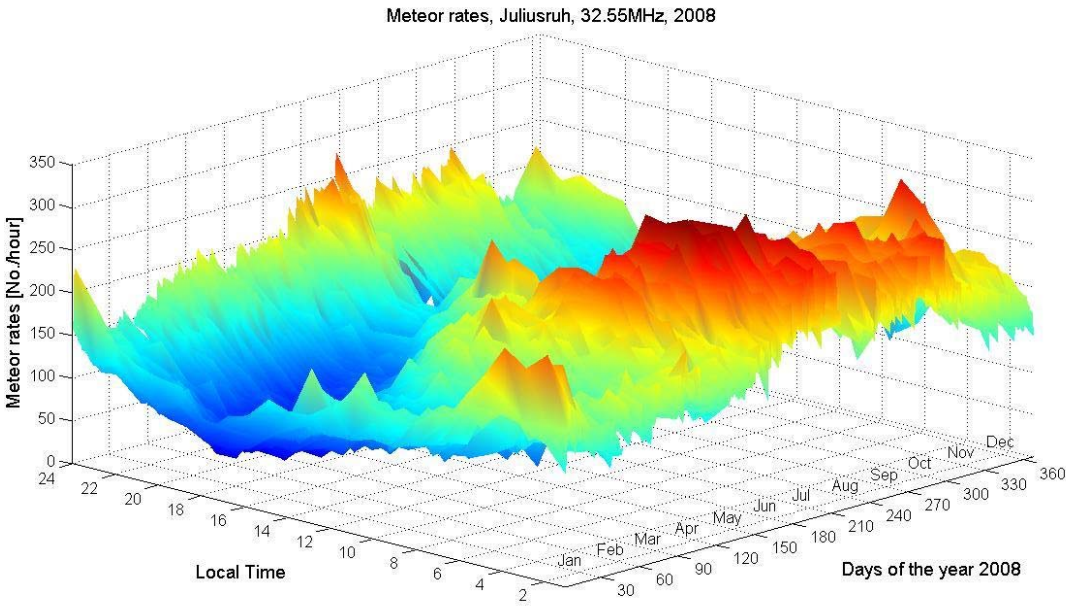

Figure 2.2 Meteor count rates variation, 54°N, 2008

Meteors also have a strong seasonal variation, which is due to the Earth's orbit around the Sun and latitude difference. Figure 2.3 shows the meteor seasonal variation observed by meteor radar on 32.55 MHz and 53.5 MHz at mid-latitude 54°N (Juliusruh) 2008. The maximum meteor rate appeared around June and July, and the minimum rate approximately in February. The dataset used in this plot include both sporadic meteors and meteor showers. There are at least two meteor showers that can be easily recognized, Quadrantids (Active: January 1~5) and Geminids (Active: December 7~17), on both radar frequencies. (International Meteor Organization 2008) Similar behaviours have also been found in the previous meteor studies.

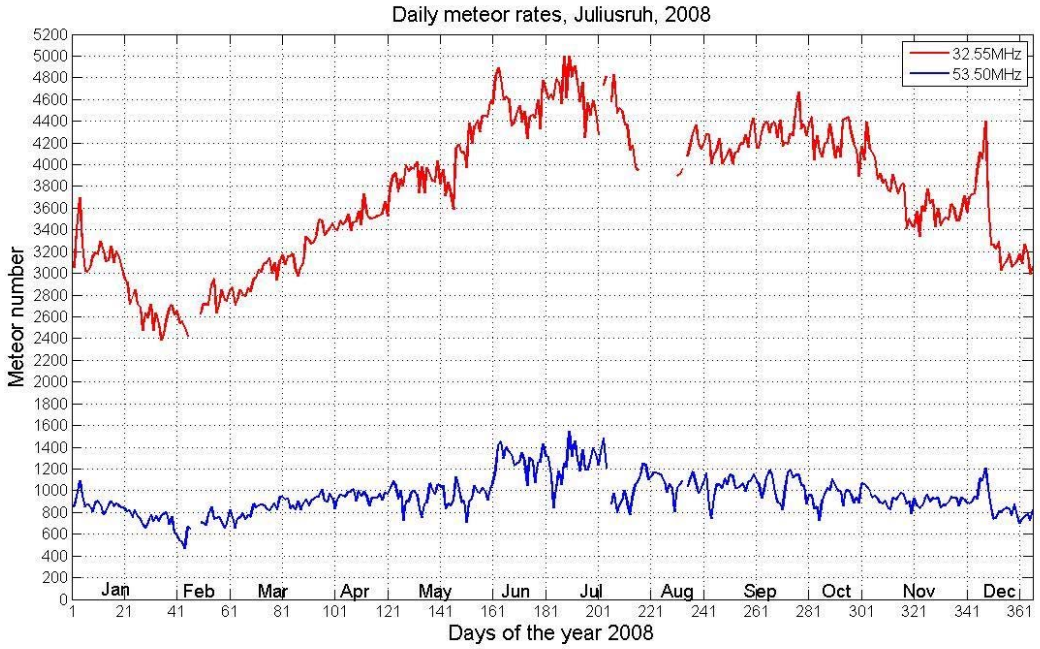

Figure 2.3 Seasonal meteor rates variation, 54°N, 2008

The location of the meteors in the sky is also one of the most important meteor parameters, which can be determined by many methods. At the same time, the height of the meteor can be calculated with the range and zenith angle of the meteor. Figure 2.4 shows the meteor height distributions for June (summertime, red-line) and January (wintertime, blue-line) at mid-latitude 54°N (Juliusruh) 2008. The significant meteor layer is at altitudes around 80~100 km, and the peak heights are about 90 km and 88 km for 32.55 MHz and 53.5 MHz respectively.

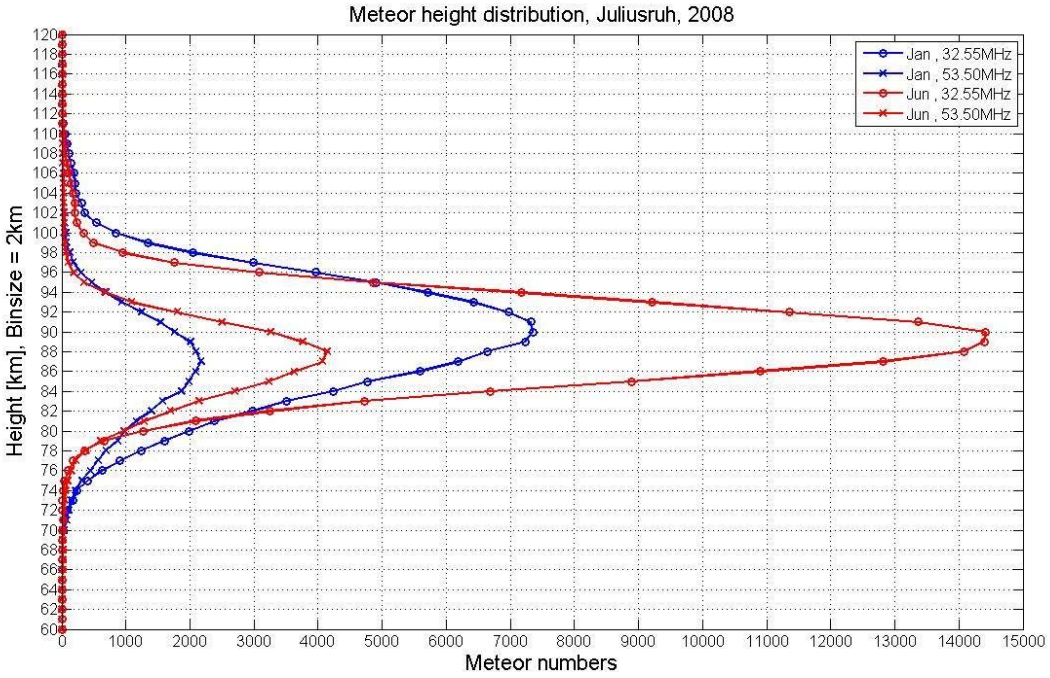

Figure 2.4 Meteor height distribution, 32.55 and 53.5 MHz, 54°N, 2008

Note that the reason for the differences between the two frequencies (32.55MHz and 53.5MHz) radar observations will be discussed in Sec. 3.3.4.

Meteors often travel at high speeds, typically 11~72 km/s. There are two useful speeds of meteors. One is the drift of the meteor trail, associated with the atmospheric wind. Another is the meteor head speed, or known as meteor entrance speed. Radar methods are mainly applied for those observations. There are more meteor parameters, like meteor radiant, meteoroid orbits, etc., which will not be discussed in the thesis. The details can be found in many books and papers. (Ceplecha et al. 1998)

2.4 Meteors and Earth's atmosphere

Mesosphere and Lower Thermosphere (MLT) are the important parts of the Earth's atmosphere where the meteor phenomenon is observed. There are many connections between meteors and the atmosphere behaviour of the atmosphere around them, e.g. wind velocity (atmospheric motion, kinetic energy), temperature (mean value around meteor layer) and atmospheric compositions. By meteor studies, the Earth's atmosphere could be understood better, and unlike the other atmosphere measurement methods, the meteor measurements provide good resolutions regardless of weather conditions. The scientists from different study fields claim that the meteor studies can show us much more information about: dynamics, composition and origin of solar system, space hazard, mass influx in the upper atmosphere, large-scale atmosphere dynamics, atmospheric entry and plasma physic, chemical process and mesospheric

layer phenomena (atomic and ion layers), etc.

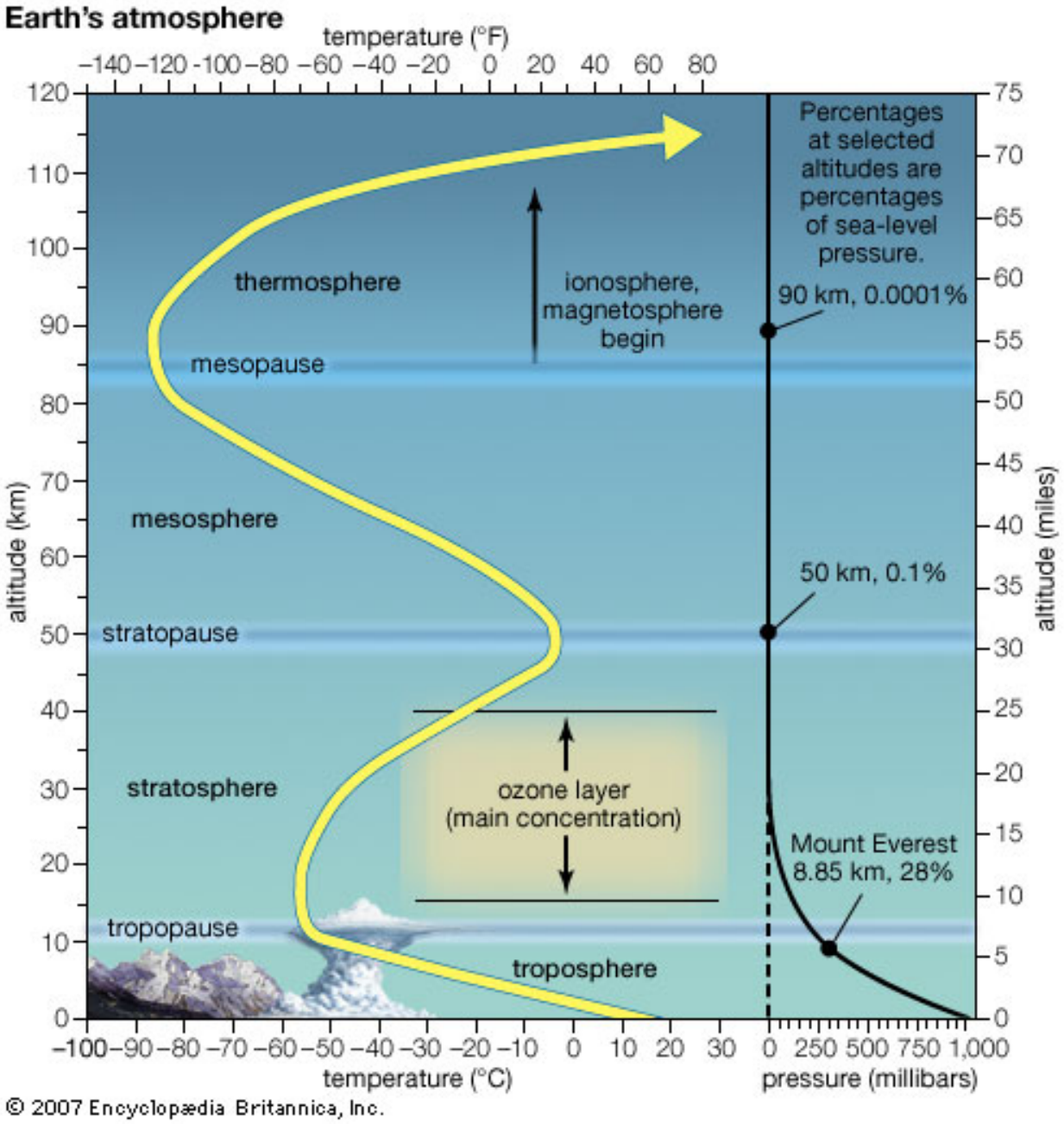

Figure 2.5 Vertical structure of the atmosphere

Earth's atmosphere is gas surrounding the Earth, which can be divided into five main layers, Troposphere, Stratosphere, Mesosphere, Thermosphere, and Exosphere. These layers are mainly determined by the vertical temperature profile. The temperature of the atmosphere has a complicated behavior by height. It starts by decreasing in the troposphere from about 290K at the ground and reaching a minimum close at 215K at 15~20 km, called the tropopause. Above the troposphere is the stratosphere, and the temperature increases again up to a maximum of close to 280K, called the stratopause (close to 50km). Above the stratosphere, the temperature decreases again in the

mesosphere and reaches the lowest temperature in the atmosphere in the mesopause, at about 70~90 km. The temperature in the mesopause may be as low as 160K or even lower at occasions. It should also be noted that the mesopause have a vertical shift during the year. The thermosphere and exosphere are the outermost layers of Earth's atmosphere extending to the outer space. (Brekke 1997)

The ionosphere is also an important layer in the atmosphere, containing charged particles, ions and electrons, produced when X-rays and UV radiation from the Sun ionizes atoms in the atmosphere. The ionospheric layers can be found at altitudes from 50 km up to 2000 km, named D, E, F1 and F2, which are shown in the right side of Figure 2.6. Those depend on the solar radiation, acting on the different compositions of the atmosphere with height. For comparison, the left side of Figure 2.6 shows the neutral atmosphere vertical structure. D-region is the portion of the ionosphere that exists approximately 50~95 km above the surface of the Earth, which covers the significant meteor layer and is the main study region in this thesis.

The electron density in the ionosphere varies on both short and long timescales. The diurnal variation happens, because the ionization occurs only during daytime, and recombination during nighttime reduces the electron density. As a result, the electron densities are higher during daytime (blue-line) and lower during nighttime (red-line), in Figure 2.6. There is also a variation with the solar cycle. During solar maximum, when the Sun's ionizing electromagnetic radiation is more intense, the electron density in the ionosphere is higher. (Kelley 1989)

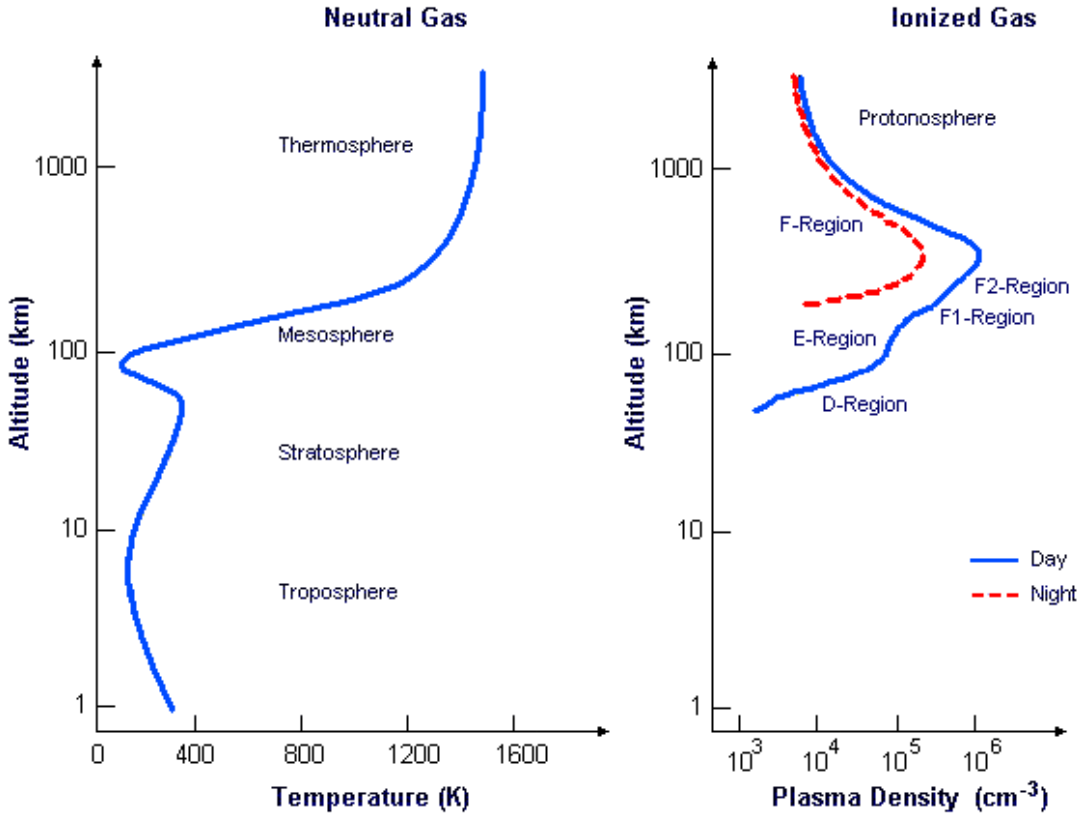

Figure 2.6 Ionosphere Height Profile (Kelley 1989)

It was known that meteors are one important source for the metal atoms in the upper atmosphere. A mass of (40 ± 20) x 106 kg/year dust enters the atmosphere with the meteor ablations. (Love and Brownlee 1993) Dust from the troposphere can only reach those heights in cases of a major volcanic eruption. (Cho, Sulzer, and Kelley 1998)

At the altitude range between 80 and 90 km in the summer polar mesopause region, ice particles are allowed to form and grow, because the temperatures are very low and the meteor dust (smoke) is assumed to act as condensation nuclei (Croskey, Mitchell, Friedrich, Torkar, Hoppe, and Goldberg 2001; Kelley, Alcala, and Cho 1998; Rapp and Lübken 1999; Seele and Hartogh 1999). The largest of these ice particles (with radii larger than 20 nm approximately) could be optically observed as noctilucent clouds (NLC), for example with the naked eye or with lidars. Figure 2.7 shows a NLC photograph by Veres Viktor, NASA. All these ice particles are immersed in the plasma of the D-region ionosphere, and electrons attach to the ice surfaces such that the particles become charged.

Figure 2.7 Noctilucent clouds (NLC), by Veres Viktor, 15th June 2007, Hungary

In addition, the 80~90 km altitude range is the region in the atmosphere where gravity waves propagating from below grow unstable and produce turbulence. The charged ice particles are transported by the turbulent velocity field leading to small-scale structures in the spatial distribution of the charged particles and, because of charge neutrality requirements, to small-scale structures in the spatial distribution of the electron number density. (Rapp and Lübken 2004)

Due to the transport of charged ice particles by the turbulent velocity field, radar waves are scattered at irregularities in the radar refractive index and very strong radar echoes could be measured on the ground, primarily in the VHF wavelength range from altitudes

close to the polar summer mesopause (Ecklund and Balsley 1981; Hoppe, Hall, and Röttger 1988; Röttger, Hoz, Kelley, Hoppe, and Hall 1988). These are known as Polar Mesosphere Summer Echoes or PMSE.

The basic physics of PMSE and NLC is quite well understood (Gadsden and Schröder 1989; Thomas 1991). It becomes clear that the observations of PMSE is a suitable tool for continuous monitoring of the thermal and dynamical structure of the mesopause region, allowing insights into important atmospheric key parameters like neutral temperatures, winds, gravity wave parameters, turbulence, solar cycle effects, and long term changes. (Rapp and Lübken 2004)

3 Radar observations of meteors

During the dark clear night, meteors can be seen. To most people, meteors only seem to show up at nighttime, but meteor phenomena are happening at every moment, daytime and nighttime, which usually can't be seen by human eyes.

A long time ago, scientists started to explore the meteor phenomena in the atmosphere. Different observation methods were developed, which yield data from the geometry of the atmospheric trajectory, the dynamics and ablation of the body in the atmosphere, radiation, the spectral distribution of radiation, ionization, sounds and orbits.

Every moment, a large number of meteors burn up in the upper atmosphere around altitudes 70~120 km. These heights are too high for *in situ* observations of meteors from aircrafts or balloons and too low for satellites or space stations. The sounding rocket measurements are the only alternative for *in situ* measurement, which are sophisticated and expensive. So, remote sensing, particularly radar techniques, is the most effective method to explore the atmosphere at those altitudes. The common meteor observation methods, results and requirements are summarized in the following Table 3.1.

Table 3.1 Meteor observation methods

Methods	**Results**	**Requirements**
Visual observations (Naked-eye)	Meteor rates, magnitude, trail duration, orientation	Nighttime observation, good weather condition, brighter meteors
Photographic observations	Trail position, orientation, angular velocity	Nighttime observation, good weather condition
Television and video observations	Meteor rates, magnitude, trail duration, orientation	Nighttime observation, good weather condition
Spectral observations	Meteor spectrum	Nighttime observation, good weather condition
Radar observations	Meteor rates, magnitude, trail duration, orientation, velocity, etc.	No particular requirements
Acoustic, infrasonic, and seismic observations	Meteor rates	No other sound and vibration sources
Combined observation methods	Combined results	Depending on the individual observation methods

Radar techniques are very useful and powerful tools for the studies of the Earth's atmosphere and ionosphere. In particular, for continuous observations in certain regions, it is really hard with other techniques, e.g. aircrafts, balloons, rockets or satellites. Radar, as a feasible remote sensing method, is very sensitive to meteors (as faint as 10~15

magnitudes) and ionization phenomenon (meteor trails). Also radar is able to work for 24 hours and in all weather conditions. So, in modern meteors studies, the combination of radar observations and in-situ measurements, assisted with models and simulations, is widely applied, which yields the most complete view of the Earth's middle and upper atmosphere and ionosphere environment. (McKinley 1961; Röttger 2004)

3.1 All-sky meteor radar

Classical interferometric SKiYMET radars, which have almost identical hardware and software, are used in this study. The following Table 3.2 shows the radar system setup used in the measurements.

Table 3.2 Basic instrument parameters

Frequency	32.55 MHz or 53.5 MHz
Peak power	12 kW
Pulse width	13 μs
Pulse rep. frequency (PRF)	2144 Hz
Transmitting antenna	3-element crossed Yagi antenna
Receiving antenna	5-channel interferometer of 2-element crossed Yagi antennas
Sampling resolution	0.94 ms
Height range	78-120 km
Angular resolution	2º

The system hardware contains four major elements, antennas, cables, transmitter and receiving/digitizing unit. The radar antennas apply crossed Yagi antenna elements to ensure approximately uniform azimuthal sensitivity zone. The system uses a 5-antenna interferometer on reception, resulting in a range accuracy of 2 km and angular accuracy of 1º ~ 2º in meteor location. As shown in Figure 3.1, the five receiving antennas are arranged in an asymmetric cross, with the distances of 2 or 2.5 wavelengths between each other. And the transmitter antenna (red) should be located at more than 2.5 wavelengths lengths from any of the receivers. The connect cables are separated for each receiving antenna with equal phase delay. The next hardware unit is called the Radar Data Acquisition System (RDAS), which includes five identical receivers connecting the five independent receiving antennas to the digitization system. (Hocking, Fuller, and Vandepeer 2001; Singer, Zahn, and Weiß 2004b)

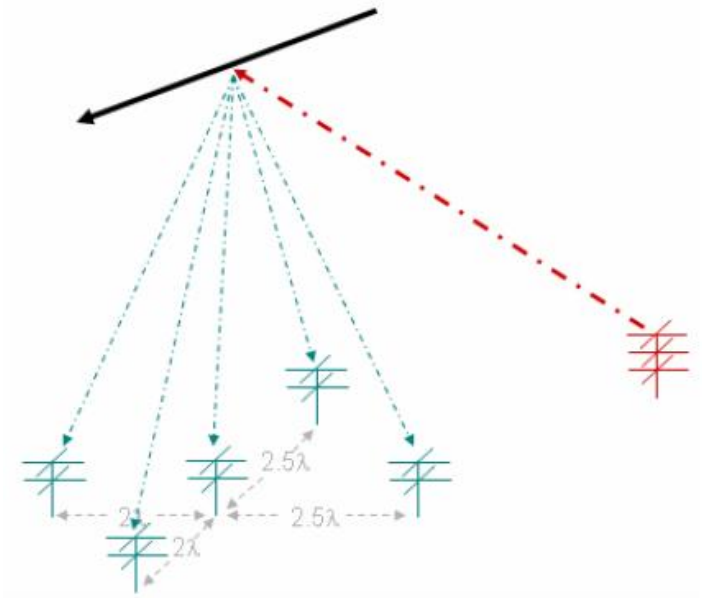

Figure 3.1 Layout of the radar field (Millan 2005)

Figure 3.2 shows more details about the detection process of all-sky meteor radar. The transmit radar sends out short pulses, which has a broad radiation pattern designed to illuminate a large extent of the sky, “all-sky”. The short-lived meteor trail forms the reflecting target for the radio waves and part of the incident energy are reflected back. The backscattered signals are received by an array of receiving antennas, and are then detected and recorded by the digital system. The receiving antenna array is arranged as an interferometer and phase differences in the signals arriving at each of the antennas of the interferometer can be used to determine an unambiguous angle of arrival. Together with range information, the position of the meteor can then be accurately located in the sky (Anon. User manual).

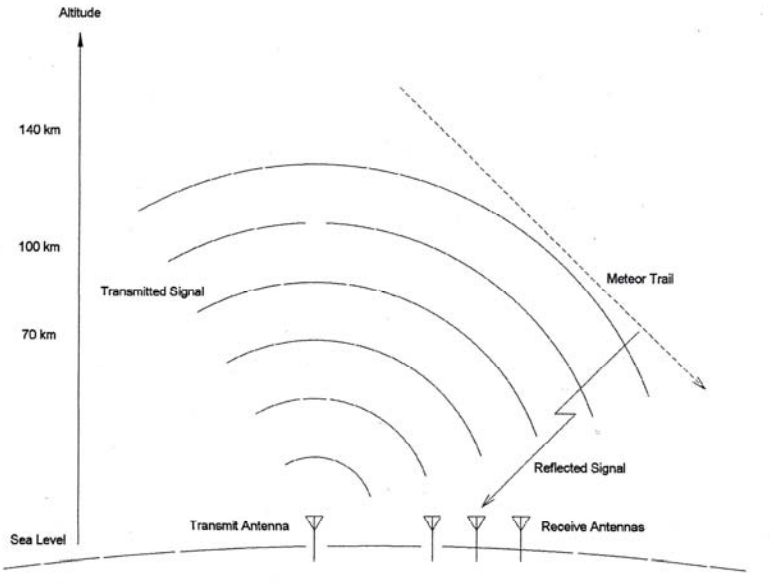

Figure 3.2 The principle of operation of the meteor radar

3.2 Underdense and overdense meteors

The meteor trails are the main targets of the radar observations in this study. The radar backscattering from meteor trails can be divided into two major groups, depending on whether the meteor trails' electron line densities are smaller or greater than a certain critical value. Very briefly, if smaller, the meteor trail is said to be underdense, the radio wave penetrates the column freely, and each electron acts as an individual scattering source. If greater, the trail is overdense, and the radio wave does not penetrate the column but is effectively reflected from that boundary surface inside which the electrons are dense enough to cause total reflection, as a local miniature ionosphere. It is very important to note that, only underdense meteors were studied in this thesis.

The meteor trail behavior and the basic model of the underdense and overdense trails are described next. When a meteoroid is penetrating the atmosphere, a stationary column of free electrons is created, with a small diameter compared to the wavelength applied by the meteor radar. The column expands radially, because of the electrons recombination, attachment, or diffusion.

The incident radio wave penetrates the column and is scattered by the individual free electrons, which oscillate freely in the applied field without colliding with other particles to any great extent. Each electron behaves as if no other was present, secondary radiative and absorptive effects may be neglected. This condition defines the *underdense trail*. If the volume density of the electrons is large enough, secondary scattering from electron to electron becomes important. The electrons are no longer independent scatterers, the incident wave does not penetrate the column freely. These are the conditions for the *overdense trail*. (McKinley 1961) The typical radar observation result of the overdense meteor is showed in Figure 3.3.

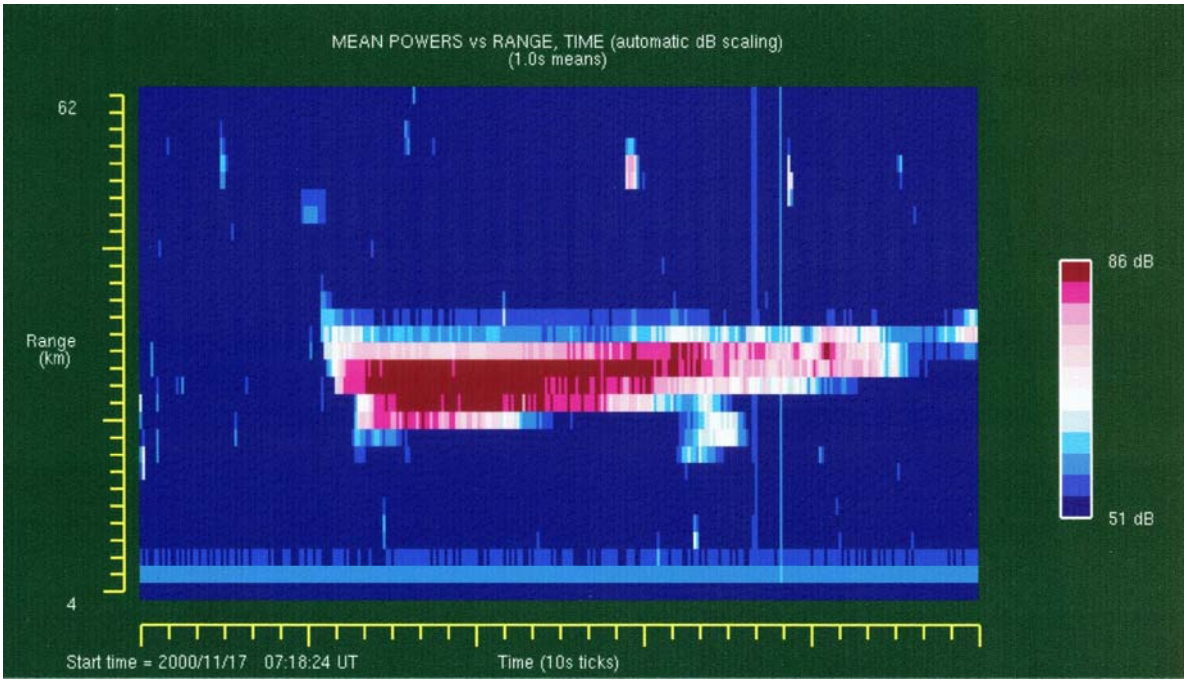

Figure 3.3 Radar observation of overdense meteor

3.3 Radar experiments

3.3.1 Primary observation

(1) Echo range: The distance from the station to the meteoric target is known as the echo range and is a fundamental measurement easily made with pulse or FM backscatter radars.

(2) Echo phase: This term is used to describe the phase of the received echo wave relative to the transmitter wave. The echo phase may be regarded as a very precise measurement of relative range.

(3) Echo amplitude or echo power.

(4) Echo polarization.

(5) Echo decay time and echo duration: The decay time τ, is defined as the time when the meteor echo amplitude reaches one-half of the peak value. Typical underdense trail echoes (shown in Figure 3.4) rise rapidly to a peak after the meteor passes the nearest point and then decay exponentially.

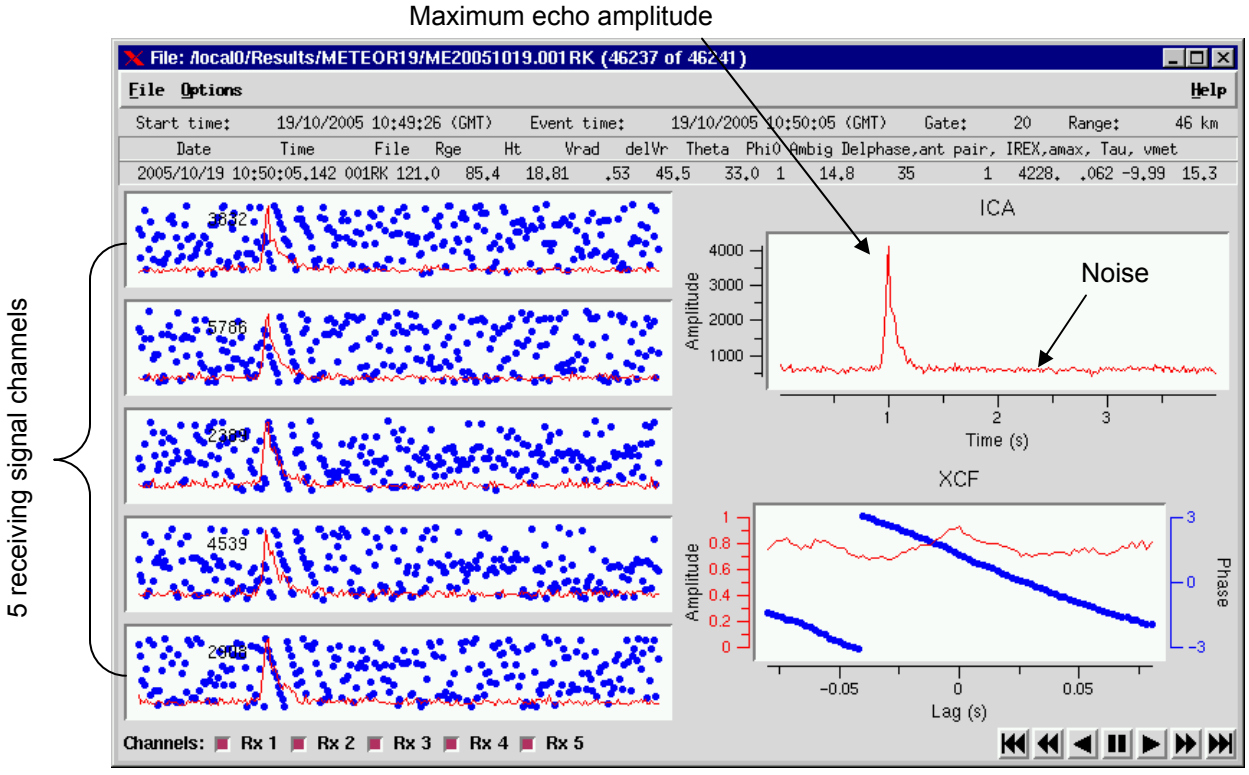

Figure 3.4 Primary observation results from the SKiYMET radar system

3.3.2 Secondary observation

From the primary observation data and the empirical models, many useful and important secondary data can be deduced, e.g. height and position of the meteor trails, atmospheric wind velocity, mean temperatures around the meteor layer, radiant location, meteor entrance speeds, etc. (McKinley 1961)

(1) Meteors height and position

The simplest method for measuring the height of the meteor trails in atmosphere is to use narrow beam radar and measure the range of the echo. But, this method requires the radar beams about 2° ~ 3° wide. Now the common technique is to use the combination of several radar ranges together to measure the direction of the reflection point by phase comparisons of signals received on closely spaced antennas. Since the range and the angle from zenith for each receiver antennas are known, the height of the meteor can be calculated. And height accuracies of 1~2 km can be expected. At the same time, meteor range and zenith angle can show the position information of meteor trail, by simple triangulation method.

In real meteor observations, there are some uncertainties, which cannot be ignored. Firstly, the radar backscattering echo should be from the same part of the meteor trail, however, most observations of the underdense trails are not like that. The zenith angle of the meteoric target may be found by comparing the echo amplitudes picked up by two antennas, which have different antenna patterns in the vertical plane. Also, there is unavoidable range ambiguity due to high Pulse Repetition Frequency (PRF). For instance, a PRF of 2144 Hz produces an aliasing range of about 70 km, so a meteor at 150 km range appears at a range of 10 km. Likewise meteors at 80 km range or 220 km range also appear at 10 km. So, the software determines the limited height range for all possible meteors. Ranges, which do not produce a height in the region 70~110 km, are rejected. (Hocking, Fuller, and Vandepeer 2001)

(2) Upper atmospheric winds

The meteor trails of expanding ionization can drift with the winds, and may also be twisted and bent. Slow variations in the echo phase will occur, which present the velocities of the upper atmospheric winds. Measurements of this parameter are accomplished by measurements of the radial velocity of every meteor detected, and then combining these measurements in an all-sky manner to determine upper level winds. The on-line all-sky least-squares fitting routine currently assumes a uniform wind **u** = (u, v, w) and then minimizes the quantity:

$$\sum_i \left[\left\{ u \cdot r_i^u \right\} - v_{ri} \right]^2 \qquad (3.1)$$

where i refers to the meteor number in a specified height and time window. Typically, such a window would cover a height region of 3~4 km, and duration of about 1.5 h. Such windows are stepped at time steps of 1 h, and height steps of 3 km. The vector r_i^u is a unit vector pointing from the radar to the ith meteor trail. The value v_{ri} is the

measured radial velocity, and $u \cdot r_i^u$ is a dot-product. (Hocking, Fuller, and Vandepeer 2001)

Because the upper wind speed is a very common parameter, and has been determined with many other types of radar, the details will not be presented here. The examples can be found in Hocking and Thayaparan (1997) or others.

(3) Atmospheric temperatures

Atmospheric temperatures around meteor layer can be estimated from the radar observations, because of the relationship between the ambipolar diffusion coefficient, the atmospheric temperature and pressure. As formula 3.2 shows, D_a is the ambipolar diffusion coefficient, T is temperature, P is pressure, and K_a is a constant that depends on the zero field reduced mobility of the gas. This equation could be extended to formula 3.3, where k is the Boltzman constant, e is the electron charge, K_0 is a constant related to the main ion of the plasma trail, and T and P remain the same. For metallic ions colliding with N_2 neutral gas molecules, $K_0 \approx 2.5\times10^{-4}$ m^2/s. When N_2^+ is the major ion, $K_0 \approx 1.9\times10^{-4}$ m^2/s. (Chilson, Czechowsky, and Schmidt 1996; Havnes and Sigernes 2005; Hocking, Thayaparan, and Jones 1997; Jones and Jones 1990)

Detailed mechanisms of the interaction among ambipolar diffusion, temperature and pressure will not be discussed here. There are many previous studies (Baggaley 2002; Ceplecha et al. 1998; Mason and McDaniel 1988).

$$D_a = K_a \frac{T^2}{P} \tag{3.2}$$

$$D_a = \frac{2kT}{e}\left(\frac{T}{273.16}\right)\left(\frac{1.103\times10^5}{P}\right)K_0 \tag{3.3}$$

It is assumed that the ambipolar diffusion coefficient is the primary factor, which causes the underdense meteor trails' expansion. And this phenomenon is represented by the exponential decays of the backscattered radar signal. In formula 3.4, A(t) is the received signal amplitude, A_0 is the amplitude value before the beginning of exponential decay, D_a is again the ambipolar diffusion coefficient, t is time and λ is the radar wavelength.

$$A(t) = A_0 \exp\left(\frac{-16\pi^2 D_a t}{\lambda^2}\right) \tag{3.4}$$

This equation can be rewritten, using the decay time definition, in the following formula 3.5. τ is the backscattered radar signal decay time measured from the meteor observations.

$$D_a = \frac{\lambda^2 \ln 2}{16\pi^2 \tau} \tag{3.5}$$

With this theory, it is possible to estimate atmospheric temperatures from meteor decay times based on models (pressure model or temperature gradient model). Hocking et al. (1999) have demonstrated application of this theory using the temperature gradient method and showed that experimental measurements using meteor decay times agree

reasonably well with CIRA (Cospar International Reference Atmosphere), as well as the pressure model technique (Holdsworth, Morris, Murphy, Reid, Burns, John, and French 2006). The methods mentioned here do not produce an absolute measure of temperature, instead mean temperatures covering a particular height range and time period are the common output. The reason is that these calculations require a considerable number of meteor data to get reasonable results.

It is possible to convert D_a to temperature if a pressure model is used, but the results may not be accurate or reliable enough. The dominant method, applying a temperature gradient model to estimate atmospheric temperature, has the same disadvantage. The typical accuracy of these measurements is of the order of 4 to 10 K, depending on circumstances. The method is more accurate, especially in the non-summer months, when the temperature gradient can be better and more reliably represented. In addition, the assumed relation (formula 3.2) is still a largely theoretical derivation, and needs stronger confirmation.

In this study, the classical SKiYLINE software has been used to estimate the temperature, applying the temperature gradient method. The temporary result from SKiYLINE (Meteor radar system SKiYMET accessory) is showed in Figure 3.5. The basic system setups can be found in Figure 3.6. The diffusion coefficient and temperature data were stored in another file, which could be used in continued studies.

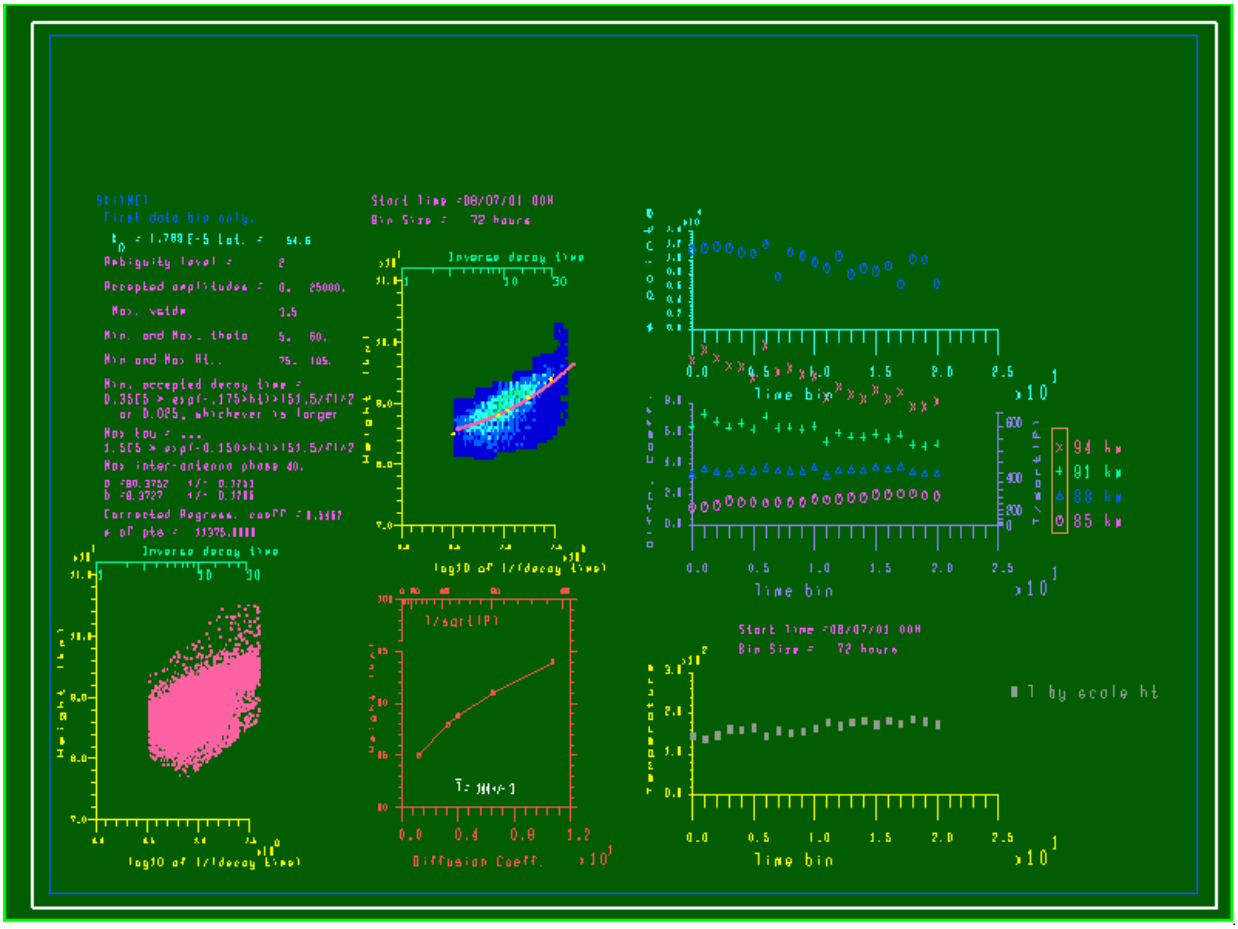

Figure 3.5 SKiYLINE result

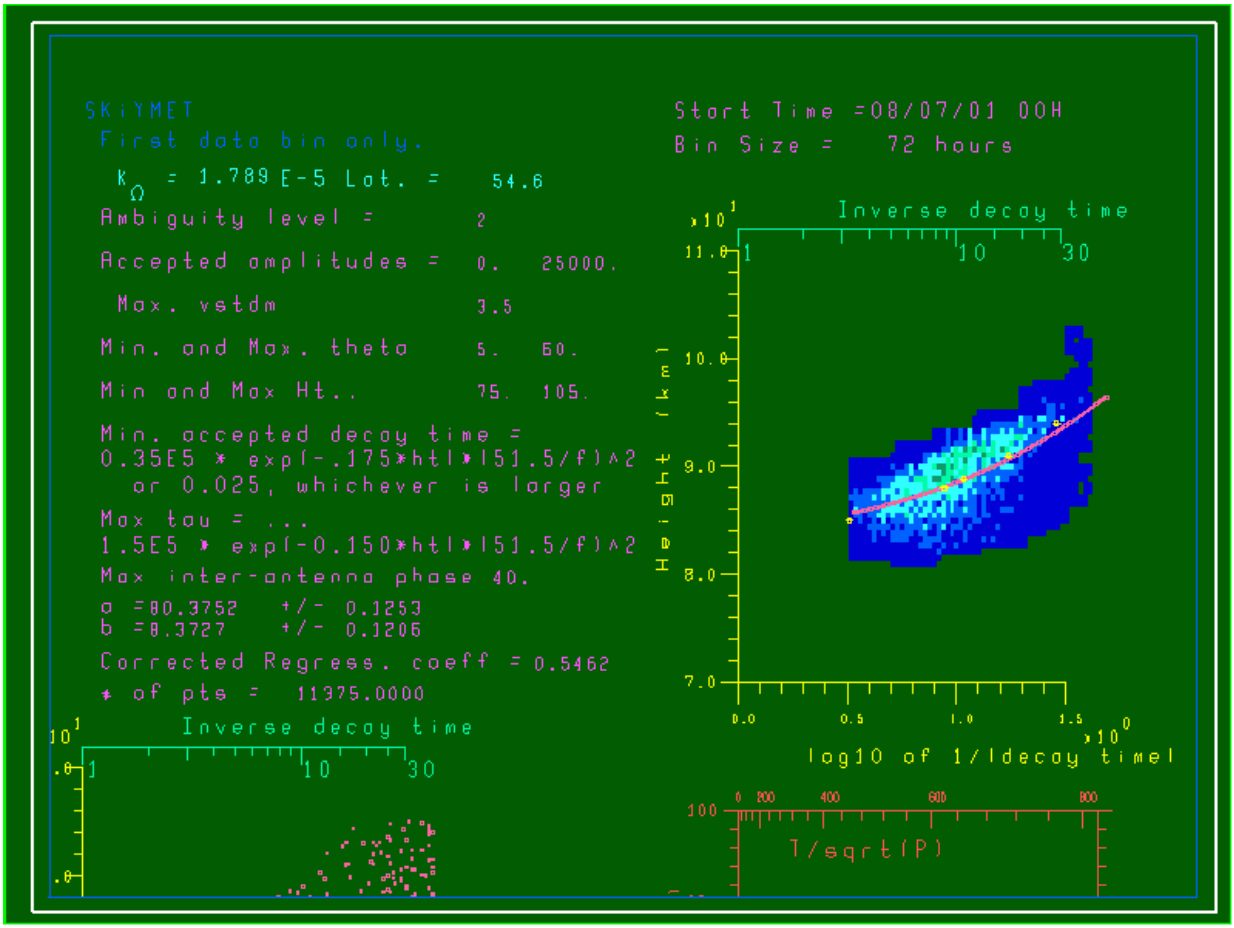

Figure 3.6 Zoom in on result from SKiYLINE

3.3.3 Characteristic results

In summary, there are many characteristic results, e.g. meteor fluxes, meteor numbers, upper atmosphere winds velocities, ambipolar diffusion coefficients, temperatures, pressures, radiant locations, meteor entrance speeds, etc.

The output results for the consecutive studies are stored in particular files for different months. First, the date and time are given (year, month, day, hour, minute, second and millisecond). Then a unique identifier is given which allows the user to identify the raw data (CEV file) for this meteor. Following this, the range and height of the meteor are listed. Then the mean radial drift velocity and its associated error for the mean are written. Following this are the angle from zenith and the azimuth angle anti-clockwise from due east. The next parameter is the ambiguity level – if this is 1, the data are unambiguous. Following this, a value representing the phase errors between antenna pairs is stored. The next parameter is a 2-digit number, which specifies which antenna pair, has this maximum phase error. Other parameters, which are written to file, include the meteor amplitude (digital units), the meteor decay time, the meteor entrance speed into the atmosphere, system signal to noise ratio (SNR), etc. (Hocking, Fuller, and

Vandepeer 2001) Figure 3.7 and 3.8 show the meteor flux and meteor rates results from the radar system at Juliusruh 54°N (32.55 MHz & 53.5 MHz).*

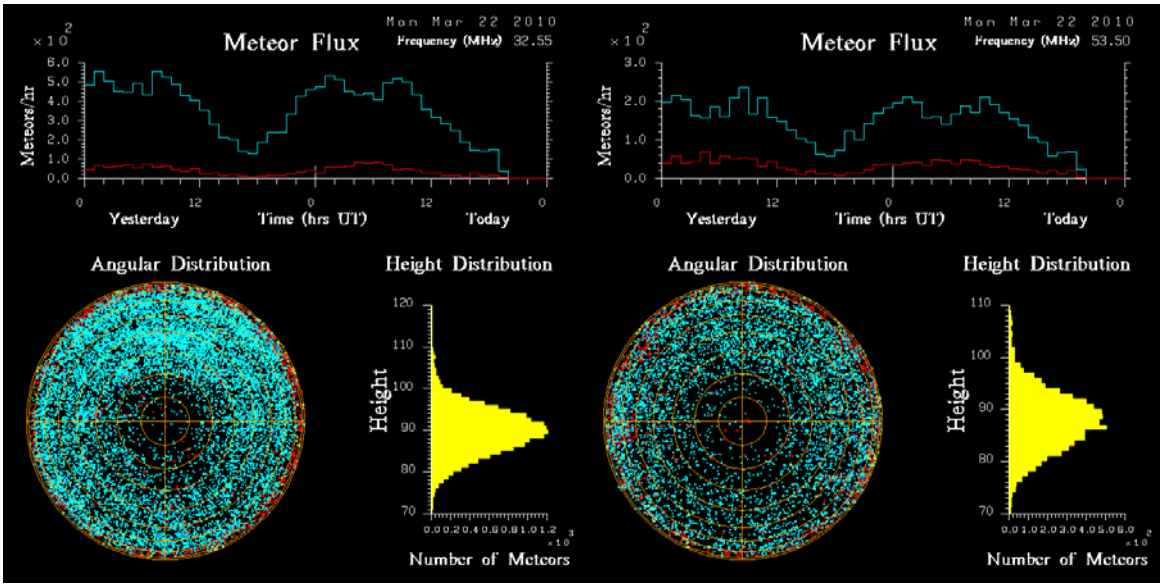

Figure 3.7 Meteor flux, Juliusruh 54°N, 32.55 MHz & 53.5 MHz

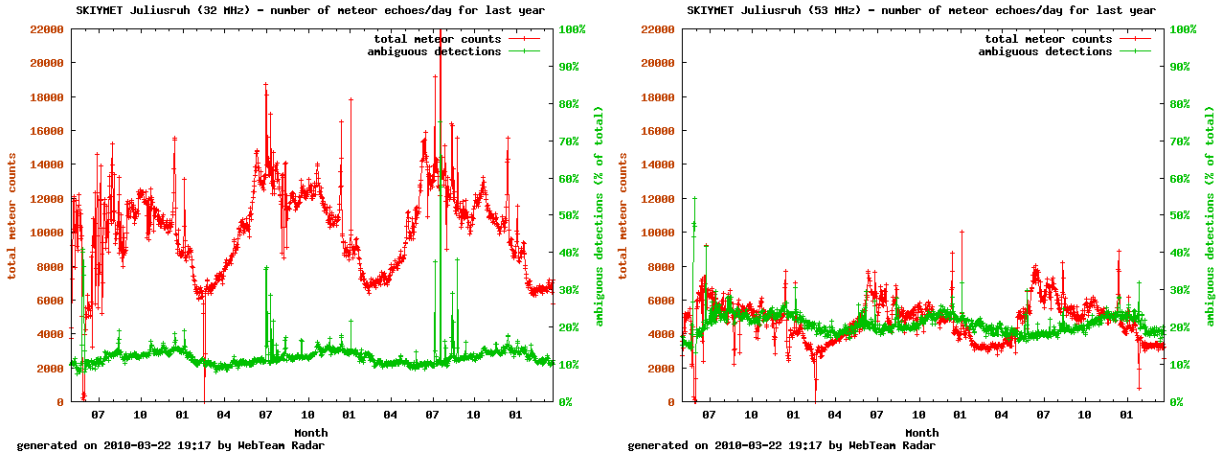

Figure 3.8 Meteor rates, Juliusruh 54°N, 32.55 MHz & 53.5 MHz

3.3.4 Comparison between meteor observations at different radar frequencies

The all-sky meteor radars are able to work with two frequencies, 32.55 MHz and 53.5 MHz. From the radio wave definition, $\lambda = c / f$ (“c” – speed of light, “λ” – wavelength, “f” –

* The results are updated in real time on the website of the Leibniz-Institute of Atmospheric Physics (IAP).
[http://www.iap-kborn.de/JMR32-Meteor-flux.257.0.html?&L=1]
[http://www.iap-kborn.de/JMR32-Meteor-rates.256.0.html?&L=1]
Visit date: March 22, 2010

frequency), the corresponding wavelengths for 32.55 MHz and 53.5 MHz are approximately 9.2166 m and 5.6075 m respectively. Comparing the observation results from both frequencies, some clear characteristics (differences) can be found.

First, meteor radar working with 32.55 MHz detects more meteors than 53.5 MHz, as shown in Figure 2.3. When the meteor trails start to expand, the shorter wavelength backscattering signals disappear first, and at high altitudes, meteor trails expand faster. With meteor observations at 53.5 MHz (shorter wavelength), it is more difficult to detect the meteors at higher latitudes, while at 32.55 MHz (longer wavelength), the meteor radars are able to detect more meteors. This also explains why the meteor sensitive heights are different between 32.55 MHz and 53.5 MHz (Figure 2.4). Longer wavelength is more sensitive at higher latitudes.

Second, according to the meteor decay time observations, we can assume that the observation results for both frequencies come from the same meteors. Then the ambipolar diffusion can be considered to be a constant. From formula 3.5, the meteor decay times are only depending on the radio frequency that the radar system applies. With those assumptions, the meteor decay times for 32.55 MHz should be 2.7 times larger than 53.5 MHz in principle.

$$\frac{\tau_{32.55\,MHz}}{\tau_{53.50\,MHz}} \approx 2.7 \tag{3.6}$$

In reality, the results are not always that simple and clear. The main uncertainty of the radar meteor observations is that current meteor observations are not able to determine the independent meteors as the assumptions said. Because of the radar system errors (range, angular, etc.), there could be several meteors at same time and position, and the difference cannot be distinguished from the radar observations. So, the mean values of meteor observation data, with particular time period or height range, are mainly applied in meteor studies.

4 Data analysis and results

4.1 Data selection

The meteor data in this study were collected from two observation stations, Juliusruh at mid-latitude 54°N and Andenes at polar latitude 69°N, where the same identical all-sky meteor radars were utilized. The radars run with two frequencies, 32.55 MHz and 53.5 MHz, but at Andenes, only the 32.55 MHz was available. The study time period is the complete year of 2008.

All the meteor data were selected by the following criteria:

i) No-data points should be checked and removed, as they probably are due to technical problems or function adjustments.

ii) Only the unambiguous meteor data were selected. The range ambiguities are caused by the high Pulse Repetition Frequency (PRF).

iii) The meteor data were also selected by the zenith angle between 10° and 60°. The meteors detected at lower elevation angles are considered to have a long path through the atmosphere, which give bad height estimations, and the meteor radar detections of the meteors close to zenith area also have bad accuracy due to the radar pattern.

iv) Strong and weak meteors (meteor echoes) were separated according to their electron line densities. The observed peak amplitudes were applied to estimate those electron line densities according to McKinley (1961, p. 189).

$$q^2 = \frac{P_R R^3}{2.5 \times 10^{-32} P_T G^2 \lambda^3} \tag{4.1}$$

Formula 4.1 shows the relation between the meteor electron line density and the meteor radar parameters, where P_R is the received echo power, P_T is the transmitted power including the feeding loss, R is the range of the meteor, G is the antenna directivity, and λ is the radar wavelength.

$$P_R = A^2 \cdot 4 \cdot 10^{-21} \tag{4.2}$$

The echo power has been calibrated by feeding defined fractions of the transmitted pulse delayed by 100 μs into the receiver instead of the antenna signal (Latteck, Singer, Kirkwood, Jönsson, and Eriksson 2005; Latteck, Singer, Morris, Holdsworth, and Murphy 2007), shown in formula 4.2, where A is the amplitude in digitizer units (P_R/W).

According to the meteor radar system used in this study, Juliusruh 54°N and Andenes 69°N, the differences of the decay times between weak and strong meteors maximize for the following electron line densities: 8.0×10^{11} ~ 1.7×10^{12} m^{-1}, 1.7×10^{12} ~ 7.0×10^{12} m^{-1}. (Singer et al. 2008) Note: Strong meteors data were mainly used in the study to minimize the background dust influences.

v) Daytime and nighttime meteor data were separated, to quest the possible influence of

the background atmospheric electron density variations. There are obvious variations between daytime and nighttime background atmospheric electron density. Daytime and nighttime were defined by Solar Zenith Angle (SZA) at the altitude 90 km above Earth's surface, where meteor layer was approximately observed. Daytime was defined with SZA<100° and Nighttime with SZA>100° in this study. The following Figure 4.1 shows the sketch of the solar position definition, where the zenith angle measured from vertical is the same definition of Solar Zenith Angle.

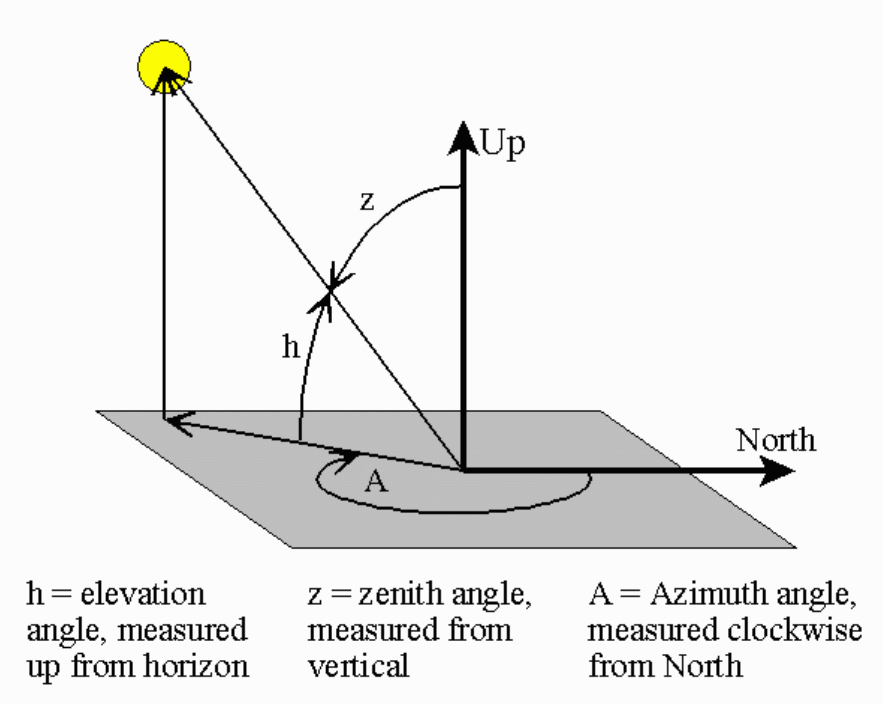

Figure 4.1 The sketch of the solar position definition

Note: In the following data processing, the meteor data normally were binned into small time periods, 3 days (72 hours) for complete year data.

4.2 Meteor decay time analysis

4.2.1 General meteor decay time behavior with altitudes

The overall observed meteor decay time variations at mid-latitude 54°N (Juliusruh) during 2008 are showed in Figure 4.2 and 4.3. Along the horizontal direction, meteor decay times have a clear seasonal variation. There was a noticeable reduction in summertime at lower altitudes. Along the vertical direction, the data are grouped into 2km height ranges, from 80 to 92 km, to find out the height-dependent trends. During most of the year 2008, the decay times showed an identical decrease with increasing altitudes, but in summertime, only at high altitudes (above 88 km for 32.55 MHz, above 86 km for 53.50 MHz).

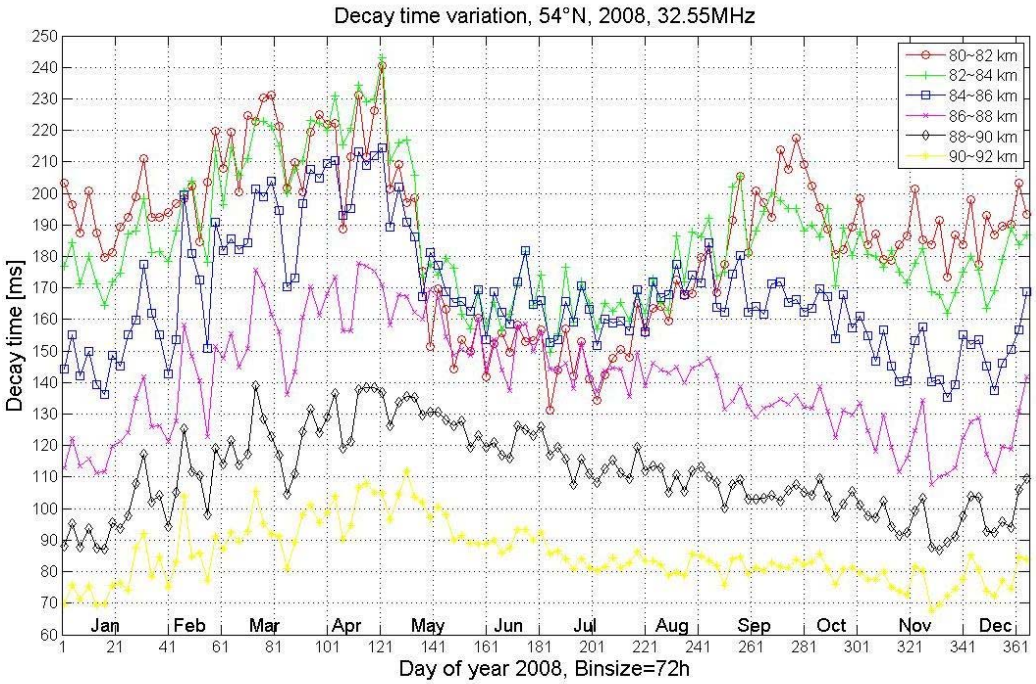

Figure 4.2 24 hours Decay time variations, 54°N, 32.55 MHz

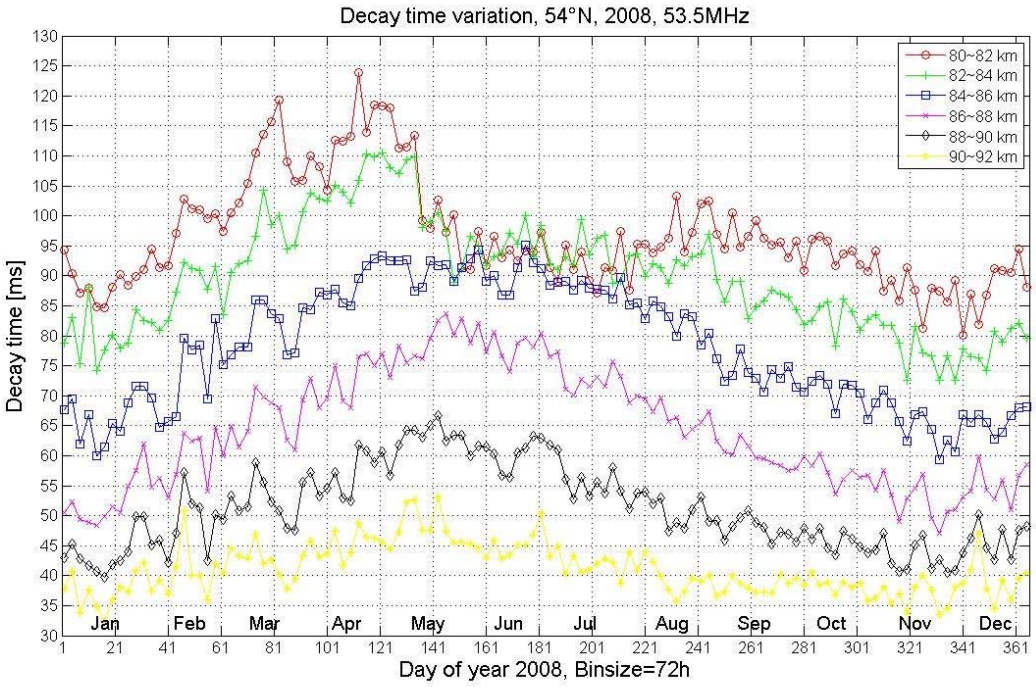

Figure 4.3 24 hours Decay time variations, 54°N, 53.50 MHz

4.2.2 Study time periods selection

For the daytime/nighttime meteor decay time comparison study, firstly it is very important to find a comparable dataset (about the same meteor numbers during daytime and nighttime) at particular time periods. In other words, approximately equivalent length of day and night is required. Figure 4.4 shows the daily meteor rate variations for daytime/nighttime at mid-latitude 54°N detected at 32.55 MHz and 53.5 MHz in 2008.

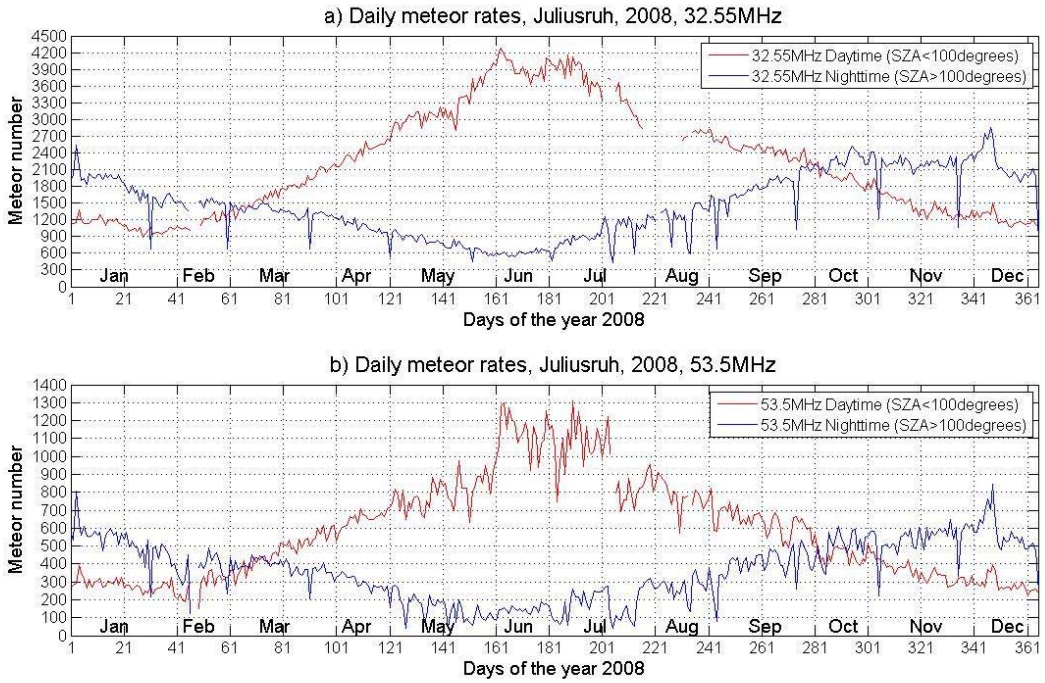

Figure 4.4 Daily meteor rates, daytime/nighttime, 54°N a) 32.55 MHz; b) 53.50 MHz

From Figure 4.4, a clear variation during the complete year can be observed, according to the daytime/nighttime length variation. The biggest difference in the meteor rates between day and night is more than 3000 meteors. From Figure 4.4, three 20 days periods of the year 2008 were selected for the day/night meteor decay time studies, day number 40~60 (Feb), 260~280 (Sep) and 280~300 (Oct).

Note: There were some gaps (no-data periods) during the observations, e.g. day number around 45 and 221, which are mainly because of technical problems or equipment adjustments during those time periods.

4.2.3 Background atmospheric electron density variations

The background atmospheric electron density variation between daytime and nighttime is considered to have a very close relationship with the meteor decay time variation. Figure 4.5 and 4.6 show the vertical variations of the background atmospheric electron

density at latitude 54°N and 69°N, covering the 3 selected periods of 2008 (Feb, Sep, Oct). Each data point is the monthly mean value of a 2 km height bin. The daytime atmospheric electron densities (red curve) are always larger than at nighttime (blue curve). The biggest difference was up to 2~3 orders of magnitude.

Note: The atmospheric electron density data are downloaded from the Internet*, then processed and plotted by Ding Tao at the Leibniz Institute for Atmospheric Physics.

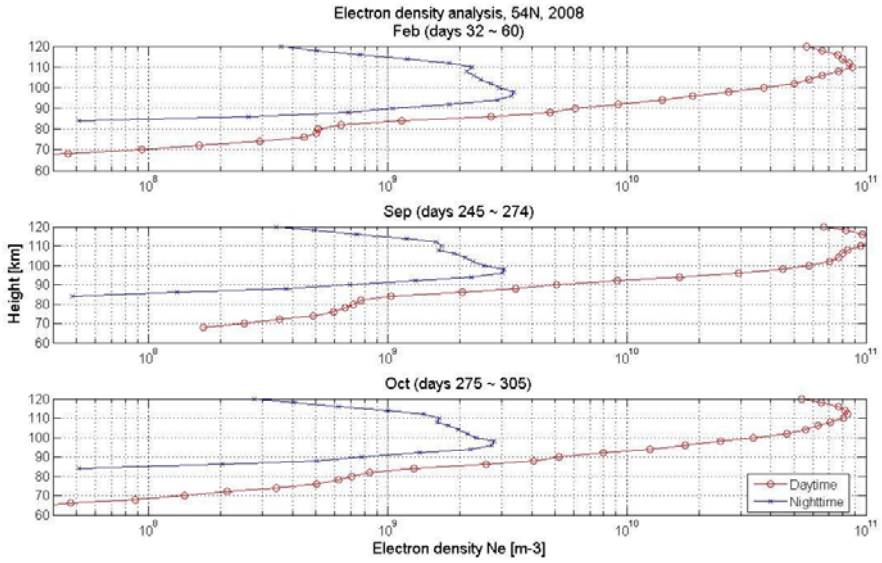

Figure 4.5 Background atmospheric electron density, 54°N

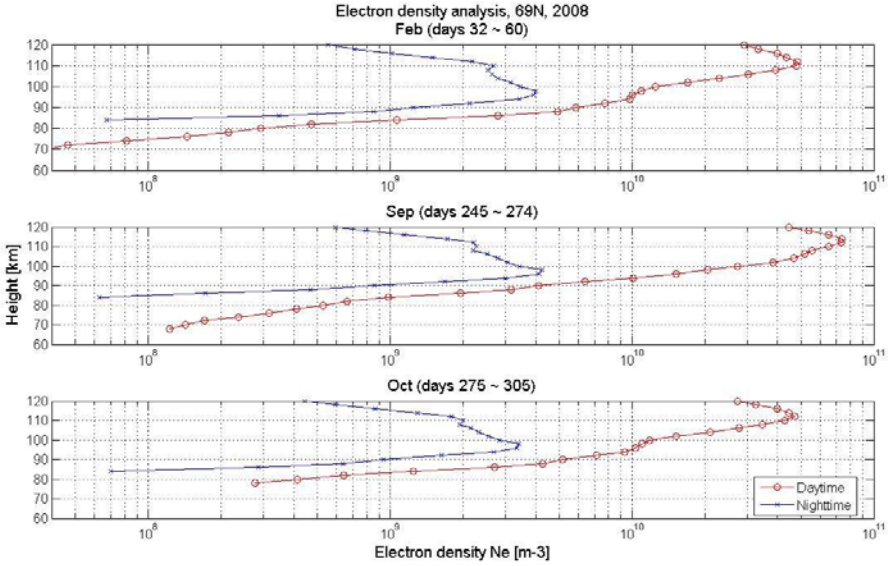

Figure 4.6 Background atmospheric electron density, 69°N

* International Reference Ionosphere (IRI – 2007) from Virtual Ionosphere, Thermosphere, Mesosphere Observatory (VITMO)
[http://omniweb.gsfc.nasa.gov/vitmo/iri_vitmo.html]
Visit date: August, 2009

4.2.4 Meteor decay time variations between daytime and nighttime

Daytime and nighttime meteor decay time comparisons for mid-latitude 54°N are presented in Figure 4.7. The mean values within the height range from 82 to 86 km were used in this plot. Generally, the meteor decay times showed the apparent difference between daytime and nighttime during the year 2008 for both frequencies. The decay times at nighttime were reduced remarkably, compared with daytime. During summertime, the daytime and nighttime decay times at 32.55 MHz overlap each other, and the differences between them are not obvious. The possible reasons could be that there are much fewer data in the summer night, and the NLC phenomenon appeared during summertime. While at 53.5 MHz, the reduced decay times during nighttime appear all the year of 2008, because the meteor radar at this frequency is more sensitive around 82~86 km.

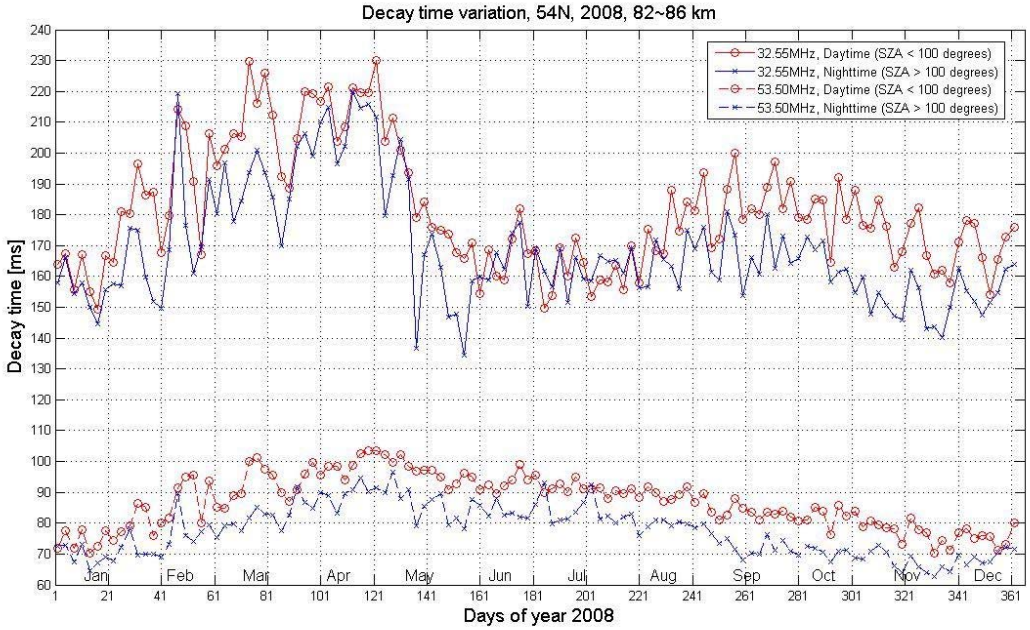

Figure 4.7 Decay time variations, daytime/nighttime, 54°N

Figure 4.8 zoom in at the 3 selected time periods with comparable data. For the frequencies 32.55 MHz and 53.5 MHz, the decay times for nighttime (low background atmospheric electron density) are reduced by up to 30% compared to daytime (high background atmospheric electron density).

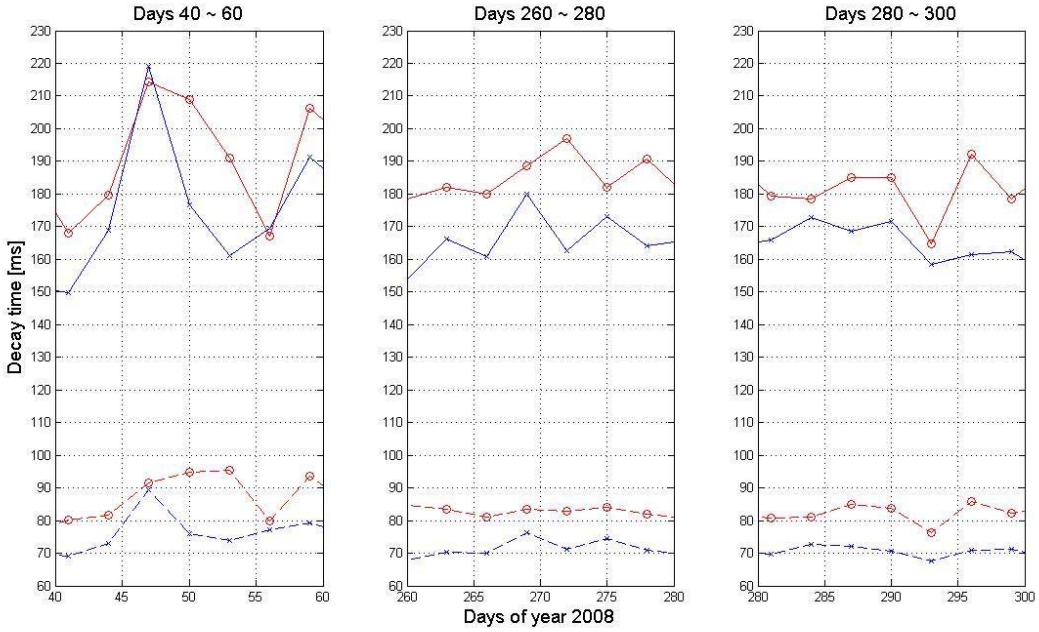

Figure 4.8 Decay time variations, daytime/nighttime, 54°N, at selected periods

The mean meteor decay times height profiles in Figure 4.9 provide more details of the meteor decay time variations between daytime and nighttime, focusing on four time periods of the year 2008, days 40~60 (Feb), days 180~200 (Jul), days 260~280 (Sep) and days 280~300 (Oct). The mean values were calculated from 2 km height ranges and 20 days time periods. Clear differences between daytime and nighttime meteor decay time were found at both 32.55 MHz and 53.5 MHz. The effect increases with decreasing height. The subplot of days 180~200 (Jul) was added to exam the meteor decay time behaviors during summertime, which shows remarkable reduction of the decay times at the lower altitudes, while during that time period (summertime), NLC phenomenon were observed around those altitudes in other studies.

The significance of the estimated mean decay time for daytime and nighttime was tested with the double-sided significance levels of the t-distribution (Taubenheim 1969). In this study, using the mean values, variances and meteor counts, most of the values reach significance levels close to 99.9%.

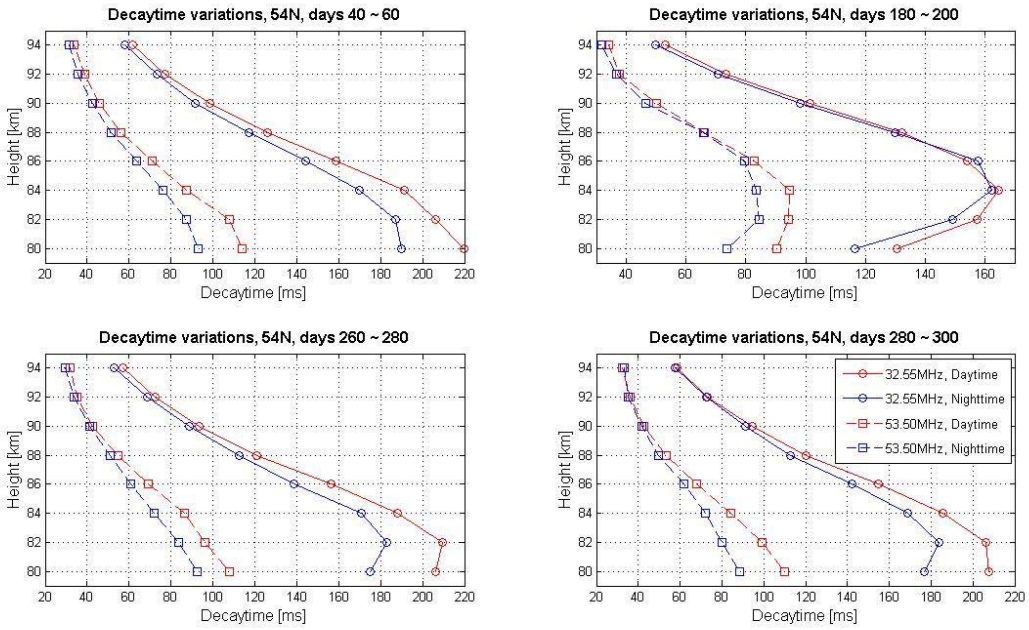

Figure 4.9 Meteor decay times height profile, 54°N

4.2.5 Polar latitude meteor decay time data analysis and results

The meteor decay time study was repeated at polar latitude 69°N (Andenes) with frequency 32.55 MHz and the results are shown in Figure 4.10 and 4.11. Compared with mid-latitude 54°N, nearly the same behaviours were found. There are much stronger seasonal variation and reduction during summertime at lower altitudes. Still, during most of 2008, the decay times showed identical decrease with increasing altitudes, except for the summertime. For the day/night meteor decay time comparison, because of the polar latitude (69°N), there are no available nighttime data during summertime. During the 3 selected periods, at daytime (high background atmospheric electron density), meteor decay times are longer than at nighttime (low background atmospheric electron density), as shown in Figure 4.12.

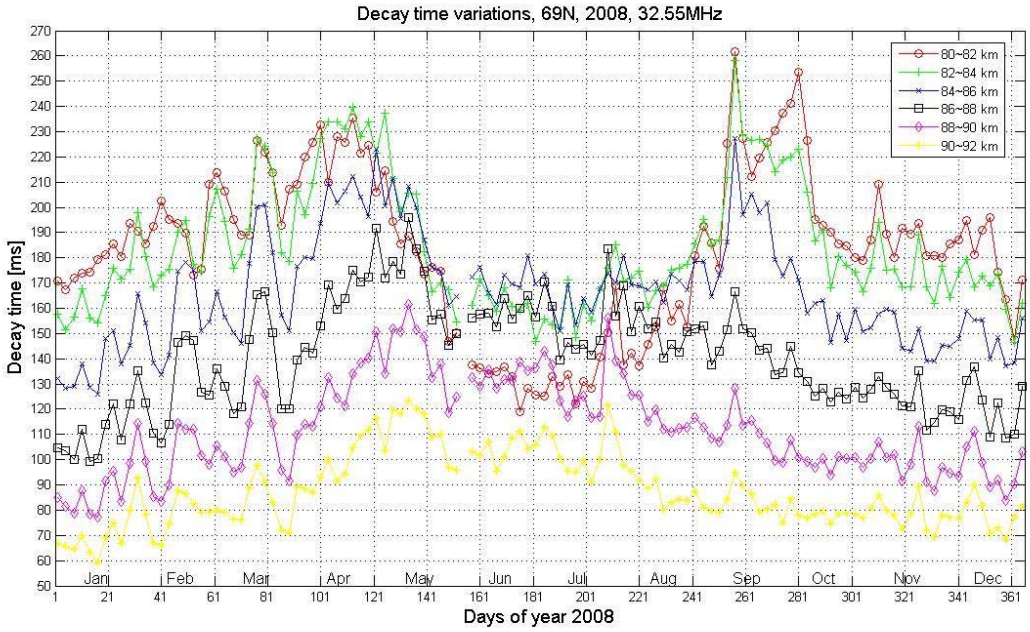

Figure 4.10 24 hours Decay time variations, 69°N, 32.55 MHz

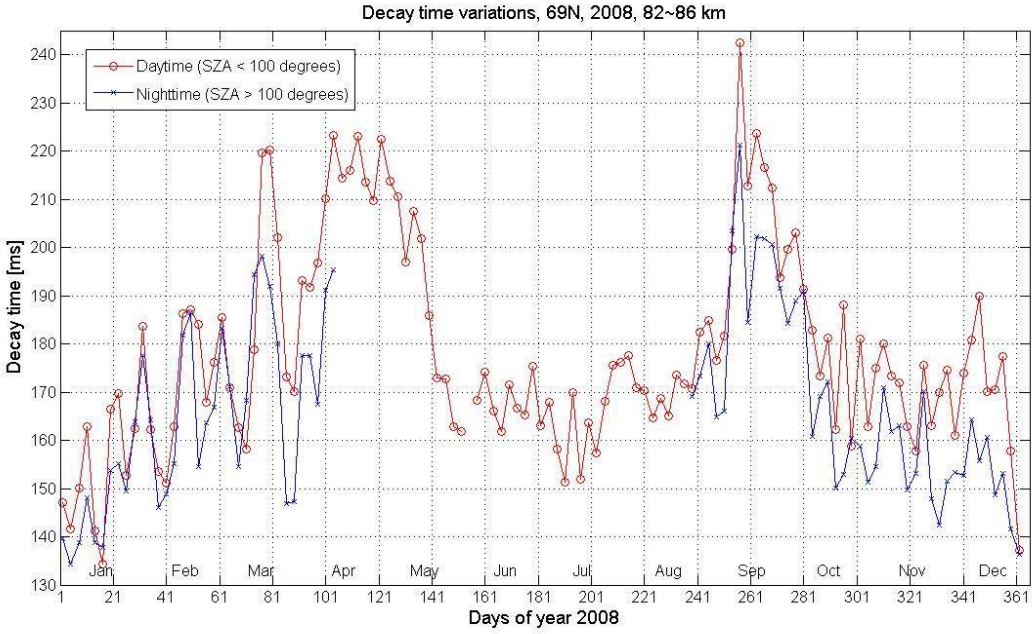

Figure 4.11 Decay time variations, daytime/nighttime, 69°N, 32.55 MHz

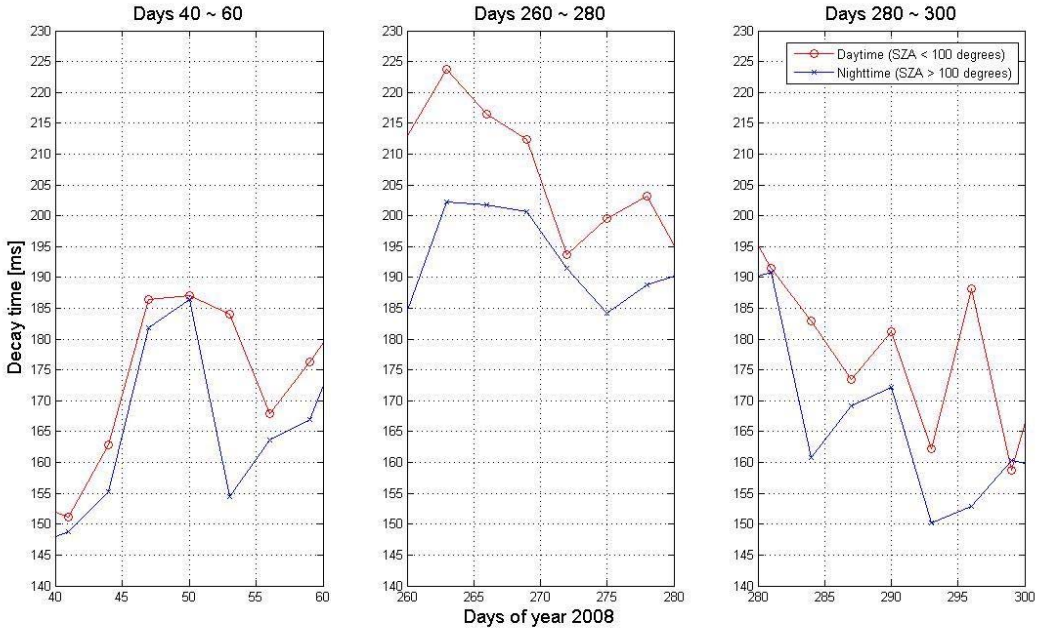

Figure 4.12 Decay time variations, daytime/nighttime, 69°N, at selected periods

4.3 Atmospheric temperature estimation

Atmospheric mean temperatures could be estimated using meteor decay times, as discussed in Sec. 3.3.2. Temperature gradient method (Hocking 1999) was applied in this study. Temperature estimation results from mid-latitude 54°N (Juliusruh) observations are mainly discussed here, because the nighttime meteor data are not available during the summertime, at polar latitude 69°N (Andenes).

To calculate the temperatures, the meteor decay time data, from all height range, were binned to 72 hours (3 days) time period. In the following Figure 4.13 ~ 4.16, three curves show the mean atmospheric temperature estimation results: (1) 24 hour mean temperatures (black) estimated from both daytime and nighttime meteor decay time data; (2) Daytime mean temperatures (red); (3) Nighttime mean temperatures (blue).

Firstly, the all-year temperature estimation results with 32.55 MHz meteor radar frequency, was showed in Figure 4.13. The estimated temperatures are clearly lower during summertime, around 145 K approximately. The curves overlap in the most of year 2008. Figure 4.14 shows the detail behaviors by zooming in at the 3 selected time periods. Normally, lower mean temperatures may be expected during nighttime, but in fact, the mean temperatures are slightly higher during nighttime than daytime in the experiment results. From Figure 4.14, especially during the days 260~280, it is clear to tell the difference between daytime and nighttime, and the difference is up to more than 12 K.

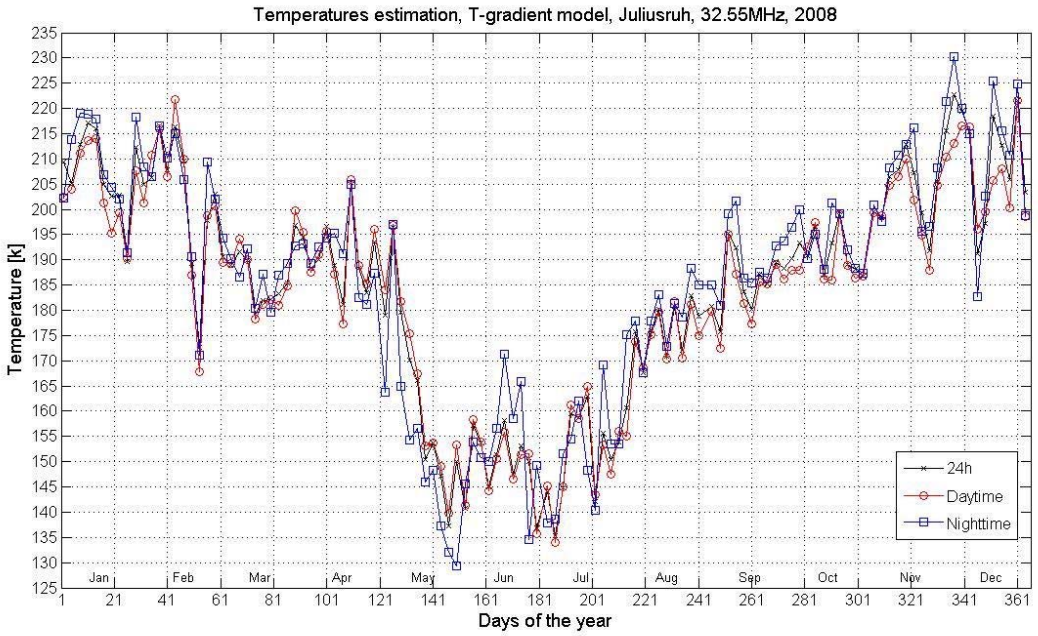

Figure 4.13 Temperature estimation result, 54°N, 32.55 MHz

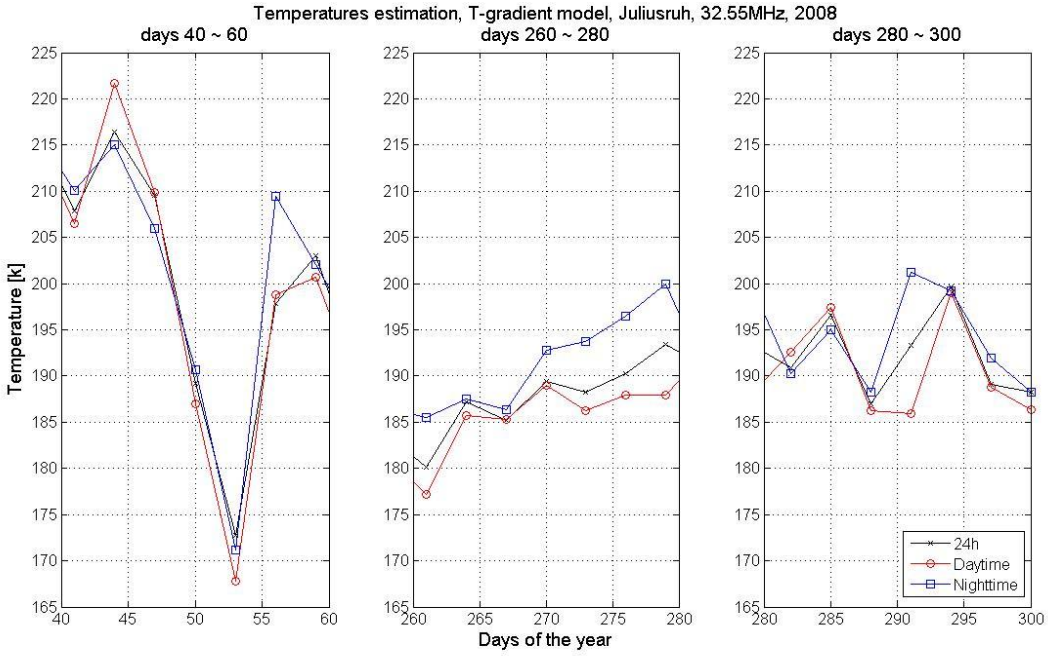

Figure 4.14 Temperature estimation result, 54°N, 32.55 MHz, at selected periods

Figure 4.15 and 4.16 show the mean temperatures estimated from meteor decay time at 53.5 MHz. Similar behaviors were observed, as well as the difference between daytime and nighttime temperature estimation results. Generally, the temperatures are slightly smaller with 53.5 MHz meteor radar frequency, because the sensitive heights for 53.5 MHz are lower than 32.55 MHz.

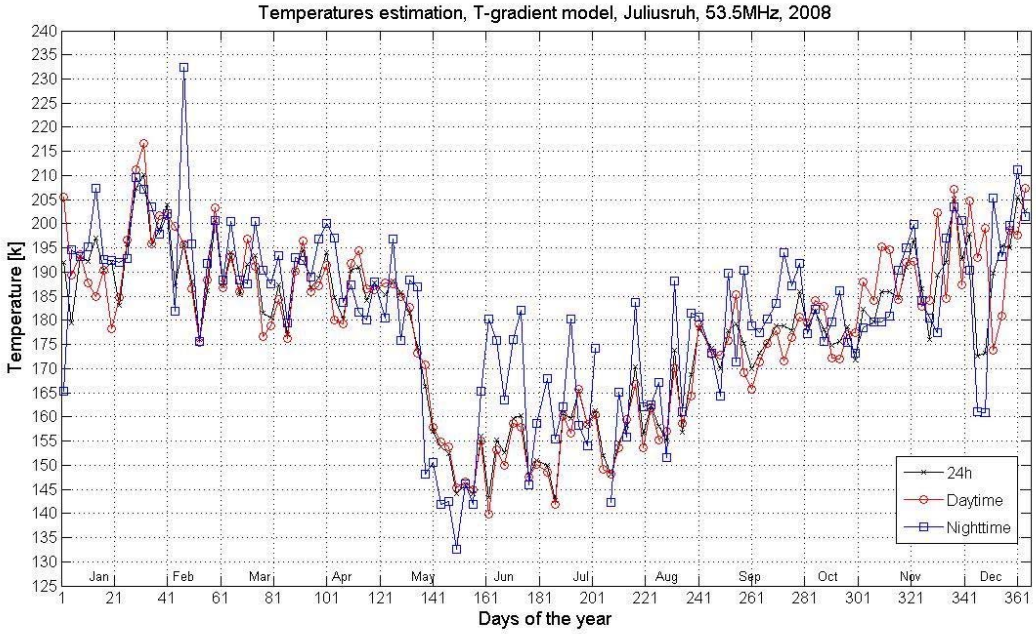

Figure 4.15 Temperature estimation result, 54°N, 53.5 MHz

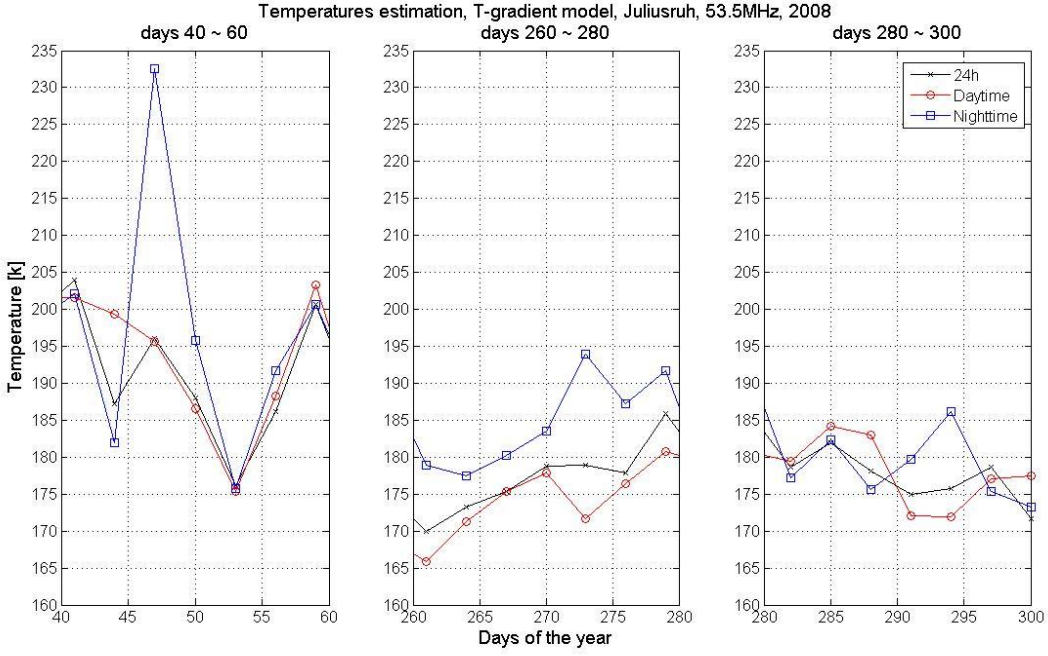

Figure 4.16 Temperature estimation result, 54°N, 53.5 MHz, at selected periods

5 Discussion and conclusions

Reduced meteor decay times were found for nighttime meteor echoes compared to daytime meteor echoes, from both 32.55 MHz and 53.5 MHz meteor radar observations, at middle and polar latitudes, most of the year 2008. Atmospheric electron density studies show variations between daytime and nighttime. This behavior generally agreed with the hypothesis, which deduced reduced meteor decay times in presence of lower background electron density.

In addition, a special behavior was found in summer with the reduction of all decay times at the lower altitudes, shown in Figure 4.2, 4.3 and 4.9. This behavior represents the vertical shift of the mesopause during the year. This is probably related to the presence of larger icy particles in the lower part of the cold summer mesopause region where the Polar Mesosphere Summer Echoes (PMSE) phenomenon occurred and the noctilucent clouds (NLC) layers were formed.

In summary, the radar observations of meteor trails showed close relations between meteor decay times and the background atmospheric electron density around the meteor layer. Because of the background atmospheric electron density variations between daytime and nighttime, the meteor decay time daytime/nighttime comparative study deduced that longer meteor decay times are usually present with larger (daytime) background electron densities, and vice versa. Lately, Dr. W. Singer et al. (2008) have showed reduced decay times in presence of neutral or positively charged dust, due to absorption of meteor trail electrons. By combining those two experimental studies, we have a comprehensive understanding of the possible influences on meteor decay times. Since the meteor decay time variations affect the temperature estimations to a large extent, more reliable temperature estimation results could be expected in future studies.

The meteor radar observations apply two radar frequencies (32.55 MHz and 53.5 MHz), that have different sensitive altitudes (layers). By combining the observation results from two frequencies, it should be possible to get more accurate results for atmospheric temperature estimations. Because instead of applying different models (pressure model or temperature gradient model), calculations based only on the decay time data at two frequencies become feasible. The combined analysis of the observation results from two frequencies should be considered for future studies. As a global phenomenon, meteor investigations require a systemic observation network to get a worldwide view. In the future, more accurate measurements could be expected from satellite-borne observations.

References

Anon. "HF/VHF all-sky interferometric meteor radar." User manual. Genesis Software Pty Ltd, MARDOC Inc.

Baggaley, W. J. 2002. *Meteors in the earth atmosphere*. United Kingdom: Cambridge university press.

Brekke, A. 1997. *Physics of the upper polar atmosphere*. United Kingdom: John Wiley and Sons.

Campbell-Brown, M. 2007. "The meteoroid environment: shower and sporadic meteors." *in Proceedings of 'Dust in Planetary Systems', Kauai, Hawaii, USA, 26-30 September 2005* ESA SP-643:11-21.

Ceplecha, Z., J. Borovicka, W. Elford, D. Revelle, R. Hawkes, V. Porubcan, and M. Simek. 1998. "Meteor Phenomena and Bodies." *Space Science Reviews* 84:327-471.

Chilson, P. B., P. Czechowsky, and G. Schmidt. 1996. "A comparsion of ambpolar diffusion coefficients in meteor trains using VHF radar and UV lidar." *Geophysical Research Letters* 23:2745-2748.

Cho, J., M. Sulzer, and M. Kelley. 1998. "Meteoric dust on D-region incoherent scatter radar spectra." *Journal of Atmospheric and Solar-Terrestrial Physics* 60:349-357.

Croskey, C., J. Mitchell, M. Friedrich, K. Torkar, U. Hoppe, and R. Goldberg. 2001. "Electrical structure of PMSE and NLC regions during the DROPPS program." *Geophysical Research Letters* 28:1427-1430.

Ecklund, W. L. and B. B. Balsley. 1981. "Long-term observations of the arctic mesosphere with the MST radar at Poker Flat, Alaska." *Journal of Geophysical Research* 86:7775-7780.

Gadsden, M. and W. Schröder. 1989. *Noctilucent clouds*. New York: Springer-Verlag.

Havnes, O. and F. Sigernes. 2005. "On the influence of background dust on radar scattering from meteor trails." *Journal of Atmospheric and Solar-Terrestrial Physics* 67:659-664.

Hocking, W. K. 1999. "Temperatures using radar-meteor decay times." *Geophysical Research Letters* 26:3297-3300.

Hocking, W. K., B. Fuller, and B. Vandepeer. 2001. "Real-time determination of meteor-related parameters utilizing modern digital technology." *Journal of Atmospheric and Solar-Terrestrial Physics* 63:155-169.

Hocking, W. K., T. Thayaparan, and J. Jones. 1997. "Meteor decay times and their use in determining a diagnostic mesospheric temperature-pressure parameter: methodology and one year of data." *Geophysical Research Letters* 24:2977-2980.

Holdsworth, D. A., R. J. Morris, D. J. Murphy, I. M. Reid, G. B. Burns, W. John, and R. French. 2006. "Antarctic mesospheric temperature estimation using the Davis mesosphere-stratosphere-troposphere radar." *Journal of Geophysical Research* 111.

Hoppe, U.-P., C. Hall, and J. Röttger. 1988. "First observations of summer polar

mesospheric backscatter with a 224 MHz radar." *Geophysical Research Letters* 15:28-31.

International Meteor Organization. 2008. "Meteor shower calendar 2008." *Journal of the international meteor organization*.

Jones, J. and P. Brown. 1993. "Sporadic meteor radiant distributions: orbital survey results." *Mon. Not. R. Astron. Soc* 265:524-532.

Jones, W. and J. Jones. 1990. "Ionic diffusion in meteor trails." *Journal of Atmospheric and Solar-Terrestrial Physics* 52:185-191.

Kelley, M. C. 1989. The Earth's Ionosphere: Plasma Physics and Electrodynamics. San Diego: Academic Press.

Kelley, M. C., C. Alcala, and J. Cho. 1998. "Detection of a meteor contrail and meteoric dust in the Earth's upper mesosphere." *Journal of Atmospheric and Solar-Terrestrial Physics* 60:359-369.

Latteck, R., W. Singer, S. Kirkwood, L.O. Jönsson, and Hakan Eriksson. 2005. "Observation of mesosphere summer echoes with calibrated VHF radars at latitudes between 54°N and 69°N in summer 2004." *in Proceedings of the 17th ESA Symposium on European Rocket and Balloon Programmes and Related Research, Sandefjord, Norway, 30 May - 2 June 2005* ESA SP-590:121-126.

Latteck, R., W. Singer, R. J. Morris, D. A. Holdsworth, and D. J. Murphy. 2007. "Observation of polar mesosphere summer echoes with calibrated VHF radars at 69° in the Northern and Southen Hemisphere." *Geophysical Research Letters* 34:L14805.

Love, S. and D. Brownlee. 1993. "A direct measurement of the terrestrial mass accretion rate of cosmic dust." *Science* 62:550-553.

Mason, E. and E. McDaniel. 1988. *Transport properties of ions in gases*. New York: John Wiley and Sons.

McKinley, D. W. R. 1961. *Meteor Science and Engineering*. New York: McGraw-Hill Book Company, Inc.

Millan, L. F. 2005. "Experimental study of the influence of background dust on radar backscatter from meteor trails." Department of Radio and Space Science, Chalmers University of Technology, Gothenburg.

Rapp, M. and F.-J. Lübken. 1999. "Modeling of positively charged aerosols in the polar summer mesopause region." *Earth planets space* 51:799-807.

Rapp, M. and F.-J. Lübken. 2004. "Polar mesosphere summer echoes (PMSE): review of observations and current understanding." *Atmospheric Chemistry and Physics* 4:2601–2633.

Röttger, J. 2004. "Ionosphere and atmosphere research with radars." *Geophysics and Geochemistry* 6.16.5.3.

Röttger, J., C. L. Hoz, M. C. Kelley, U.-P. Hoppe, and C. Hall. 1988. "The structure and dynamics of polar mesosphere summer echoes observed with the EISCAT 224 MHz radar." *Geophysical Research Letters* 15:1353-1356.

Seele, C. and P. Hartogh. 1999. "Water vapor of the polar middle atmosphere: Annual variation and summer mesosphere conditions as observed by ground-based microwave spectroscopy." *Geophysical Research Letters* 26:1517-1520.

Singer, W., J. Bremer, J. Weiß, W. K. Hocking, J. Hoffner, M. Donner, and P. Espy. 2004a. "Meteor radar observations at middle and Arctic latitudes Part 1: mean temperatures." *Journal of Atmospheric and Solar-Terrestrial Physics* 66:607-616.

Singer, W., R. Latteck, L. F. Millan, N. J. Mitchell, and J. Fiedler. 2008. "Radar Backscattering from Underdense Meteors and Diffusion Rates." *Earth Moon Planet* 102:403-409.

Singer, W., U. von Zahn, and J. Weiß. 2004b. "Diurnal and annual variations of meteor rates at the arctic circle." *Atmospheric Chemistry and Physics* 4:1355-1363.

Taubenheim, J. 1969. Statistische Auswertung geophysikalischer und meteorologischer Daten. Germany: Geest & Portig.

Thomas, G .E. 1991. "Mesopheric clouds and the physics of the mesopause region." *Reviews of Geophysics* 29:553-575.